

**HYDROGEN PRODUCTION FROM ETHANOL
OVER SILICA SUPPORTED Cu AND Zn OXIDE
CATALYSTS**

**A Thesis Submitted to
the Graduate School of Engineering and Science of
İzmir Institute of Technology
in Partial Fulfillment of the Requirements for the Degree of**

MASTER OF SCIENCE

in Chemical Engineering

**by
Habibe Işıl TEZEL**

**February 2006
İZMİR**

We approve the thesis of **Habibe Işıl TEZEL**

Date of Signature

.....
Asst. Prof. Dr. Fikret İNAL
Supervisor
Department of Chemical Engineering
İzmir Institute of Technology

28 February 2006

.....
Assoc. Prof. Dr. Selahattin YILMAZ
Department of Chemical Engineering
İzmir Institute of Technology

28 February 2006

.....
Prof. Dr. Levent ARTOK
Department of Chemistry
İzmir Institute of Technology

28 February 2006

.....
Prof. Dr. Devrim BALKÖSE
Head of Department
İzmir Institute of Technology

28 February 2006

.....
Assoc. Prof. Dr. Semahat ÖZDEMİR
Head of the Graduate School

ACKNOWLEDGEMENTS

I would very like to express my gratitude to my Asst. Prof. Fikret İnal for he guided me throughout the whole study patiently and he helped me to complete the research and write this thesis. I would like to thank to Asst. Prof. Erol Şeker for him help and encouragement.

I would also like to thank my family for their patience, trust and endless support through all my life.

I also wish to express my great appreciation to my friends, Emrah, Hilal, Senem, Ömer and Öñiz for their irreplaceable encouragement, good humor and partnership. I must also say a special thank you to my high school friends for their deepest friendship, and another special thank you to Ömer and Öñiz for inciting me to prepare the thesis format far long time ago.

This study was supported by TÜBİTAK MİSAG-241. TÜBİTAK BAYG is kindly appreciated for the M.S. scholarship.

ABSTRACT

The majority of current energy needs are supplied by combustion of non-renewable energy sources such as fossil fuels, which is associated with release of large quantities of greenhouse gases, especially carbon dioxide and other harmful emissions to the atmosphere. The gradual depletion of these fossil fuels reserves and efforts to combat pollution and greenhouse gas emissions have generated a considerable interest in using alternative sources of energy. Ethanol used in the hydrogen production process by steam reforming.

The purpose of this work was to design a high performance catalyst for the production of hydrogen from steam reforming of ethanol. Ethanol steam reforming reaction is an endothermic reaction of ethanol with water to produce hydrogen and carbon dioxide. The different ZnO loading supported SiO₂ catalyst and Cu promoted ZnO/SiO₂ catalysts were prepared single step sol-gel method with different Cu loading.

All catalysts were characterized by X-ray diffraction, BET surface area measurements and pore diameter analysis. BET surface area decreased and average pore diameter increased as the ZnO loading increased. Based on the XRD findings, it seems that zinc silicate crystallite phase is not formed under the preparation conditions used in this dissertation.

The activity and selectivity tests of all catalysts were performed in a packed bed reactor with reaction temperature between 300 and 500°C. The performances of ZnO/SiO₂ catalysts in ethanol steam reforming reaction were investigated as a function of ZnO loading. Cu catalysts are known as active catalysts for ethanol dehydrogenation. As the temperature was increased, the conversion increased and reached a maximum at 500°C for all Cu loadings.

ÖZET

Günümüzde en önemli enerji kaynağı fosil yakıtlardır fakat fosil yakıt yataklarındaki azalma ve bunların kullanımının atmosfer üzerindeki olumsuz etkisi temiz enerji konulu araştırmalara hız kazanmıştır. Etanoldan üretilen hidrojen yakıt hücrelerinde kullanıldığında hem verimli enerji üretilmekte hem de doğada kapalı bir karbon çevrimi oluşturulmaktadır.

Bu çalışmanın amacı etanoldan buhar riformlaması tepkimesinde yüksek performans sağlayacak katalizör tasarlamaktır. Etanol buhar riformlaması endotermik bir tepkimedir, hidrojen ve CO₂ üretilir. Silikanın üzerine farklı ZnO ve Cu yükleyerek katalizör sentezlenmiştir.

Sentezlenen bütün katalizörler XRD ve BET analizleri ile karakterize edilmiştir. BET analizinde, ZnO yüklemesi arttığında yüzey alanının azaldığı görülmüştür. XRD analizinde de çinko silikat kristalleri görülmemiştir.

Hazırlanan bütün katalizörlerin aktivite ve seçimlilik testleri dolgu yataklı reaktörde 300 ve 500°C arasında yapılmıştır. Etanolun buhar riformlaması deneyinde, farklı ZnO eklemelerinde, ZnO/SiO₂ katalizörünün performansı ayrıca Cu eklenmiş katalizörlerinde performansı incelenmiştir. Bütün katalizörler için, sıcaklıkla beraber aktivitenin arttığı gözlenmiştir.

TABLE OF CONTENTS

| | |
|---|------|
| LIST OF FIGURES | vii |
| LIST OF TABLES | viii |
| CHAPTER 1. INTRODUCTION | 1 |
| CHAPTER 2. LITERATURE REVIEW | 7 |
| 2.1. Thermodynamic Analysis Studies..... | 7 |
| 2.2. Catalytic Research..... | 10 |
| CHAPTER 3. MATERIALS AND METHODS | 21 |
| 3.1. Materials..... | 21 |
| 3.2. Methods..... | 22 |
| 3.2.1. The Preparation of the Catalysts | 22 |
| 3.2.1.1. Oxide Supports | 22 |
| 3.2.1.2. Copper Doped ZnO-SiO ₂ Mixed Oxide Catalyst | 24 |
| 3.2.2. Catalyst Characterization | 25 |
| 3.2.3. The Activity Tests of the Catalysts | 25 |
| CHAPTER 4. RESULTS AND DISCUSSIONS | 28 |
| 4.1. Characterization Results..... | 28 |
| 4.2. Catalytic Activity and Selectivity Tests | 29 |
| 4.2.1. The Effect of ZnO Loading..... | 30 |
| 4.2.2. Water/Ethanol Ratio Effect on the Activity and Selectivity | 35 |
| 4.2.3. Activity of 50%ZnO-SiO ₂ Catalyst as a Function of Cu Loading..... | 38 |
| CHAPTER 5. CONCLUSIONS | 43 |
| REFERENCES | 46 |

LIST OF FIGURES

| <u>Figure</u> | <u>Page</u> |
|--|-------------|
| Figure 1.1. The schematic of a fuel cell operating with a hydrogen rich fuel and an oxidant..... | 3 |
| Figure 3.1. Schematic Diagram of the Experimental Setup for the Production of H ₂ from Ethanol..... | 26 |
| Figure 4.1. XRD spectra of single step sol-gel made catalysts as a function of ZnO loading..... | 29 |
| Figure 4.2. Ethanol conversion activity of single step sol-gel made 30%ZnO-SiO ₂ catalyst as a function of total flow rate..... | 30 |
| Figure 4.3. Ethanol conversion activities of single step sol-gel made ZnO-SiO ₂ catalysts..... | 31 |
| Figure 4.4. Effect of water/ethanol ratio on ethanol conversion activity over 50 % ZnO-SiO ₂ catalyst as a function of temperature..... | 36 |
| Figure 4.5. XRD spectra of Cu-50%ZnO-SiO ₂ catalysts as a function of copper loading..... | 39 |
| Figure 4.6. Effect of copper loading on ethanol conversion activity over Cu-50 % ZnO-SiO ₂ catalysts as a function of temperature..... | 40 |
| Figure 4.7. Carbon selectivity to carbon containing products (%) over 5%Cu-50 % ZnO-SiO ₂ catalyst as a function of temperature..... | 41 |

LIST OF TABLES

| <u>Table</u> | <u>Page</u> |
|--|-------------|
| Table 1.1. Types of fuel cells..... | 4 |
| Table 2.1. Effects of process parameters in the study of Liguras et al | 13 |
| Table 2.2. Effect of supports on H ₂ yield and CO ₂ selectivity in the study of Aupretre et al. | 18 |
| Table 2.3. Mechanisms and Products in the study of Takezawa and Iwasa..... | 18 |
| Table 3.1. Properties of chemicals used in experiments..... | 21 |
| Table 3.2. Oxide catalysts and their sol-gel preparation parameters | 23 |
| Table 3.3. Copper doped zinc oxide silica mixed oxides | 24 |
| Table 4.1. BET results | 28 |
| Table 4.2. Carbon selectivity to carbon containing products (%) over 30%ZnO-SiO ₂ catalyst as a function of temperature..... | 34 |
| Table 4.3. Carbon selectivity to carbon containing products (%) over 50%ZnO-SiO ₂ catalyst as a function of temperature..... | 34 |
| Table 4.4. Carbon selectivity to carbon containing products (%) over single step sol-gel made 70%ZnO-SiO ₂ catalyst as a function of temperature | 34 |
| Table 4.5. Carbon selectivity to carbon containing products (%) over precipitation made ZnO catalyst as a function of temperature | 35 |
| Table 4.6. Carbon selectivity to carbon containing products (%) and H ₂ yield over sol-gel made SiO ₂ catalyst at 500 °C | 35 |
| Table 4.7. H ₂ yield over 30%ZnO-SiO ₂ , 50%ZnO-SiO ₂ , 70%ZnO-SiO ₂ and also precipitation ZnO catalysts as a function of temperature | 35 |
| Table 4.8. Carbon selectivity to carbon containing products (%) 50%ZnO- SiO ₂ catalyst as a function of water/ethanol ratio and temperature | 37 |
| Table 4.9. H ₂ yield over 50%ZnO-SiO ₂ catalyst as a function of temperature and water/ethanol ratios..... | 38 |
| Table 4.10. CuO and ZnO crystallite thickness | 39 |

| | |
|--|----|
| Table 4.11. Carbon selectivity to carbon containing products (%) over 5%Cu-50%ZnO-SiO ₂ catalyst as a function of temperature | 42 |
| Table 4.12. Carbon selectivity to carbon containing products (%) over 15%Cu-50%ZnO-SiO ₂ catalyst as a function of temperature | 42 |
| Table 4.13. Carbon selectivity to carbon containing products (%) over 35%Cu-50%ZnO-SiO ₂ catalyst as a function of temperature | 42 |

CHAPTER 1

INTRODUCTION

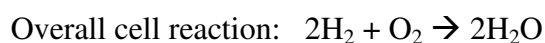
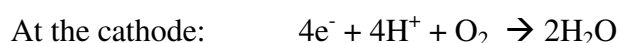
Energy demand for developing and industrialized countries has been dramatically increasing because of their high population growth rate. However, the energy supply does not increase at the same rate as the energy demand. Today's world economy is based on the fossil fuels and unfortunately the fossil fuel resources are not evenly distributed around the world. Consequently, the economies of the developing countries are affected the most due to the shortage of domestic fossil fuel supply and the dependence on the uncontrollable foreign fossil fuels. To minimize the effect, the governments of both the developed and the developing countries adopt long term strategies for future energy demands, such as promoting the usage of the alternative fuels. In addition to the economical impacts, the consumption of non-renewable fossil fuels, such as coal, releases large quantities of greenhouse gases (GHG), especially carbon dioxide (CO₂), and other harmful gases to the atmosphere. Studies have shown that the atmospheric CO₂ concentration has been increasing since the beginning of the industrialization, thus contributing to the global warming and health problems (EPA 1998). Hence, the gradual depletion of the fossil fuel reserves and the efforts to reduce the emission of greenhouse gases and other pollutants have generated a considerable interest in using alternative renewable resources in many applications (Cortright et al. 2002.; Haga et al. 1998).

Renewable energy resources could be categorized into following seven parts; Biomass, Geothermal, Hydrogen, Hydropower, Ocean, Solar, Wind. Each one has its own advantages and disadvantages. For example, solar energy is not always available throughout the day and year and also depends on the geographic location, e.g. Netherlands versus Turkey. Similarly, it is not possible to obtain reliable and constant energy from wind and ocean resources. Among these resources, hydrogen seems to be the most promising alternative resource because of the recent developments and commercialization efforts on fuel cells, especially the proton exchange membrane (PEM) fuel cell, for the generation of electric power for both electric vehicles and distributed electric power plants (Creveling 1992.; Dunison and Wilson 1994). The

major reason of the interest on hydrogen and fuel cells is the high energy efficiency of the fuel cell as compared to traditional power generations, such as power stations and vehicles (~40% for power station and <20% for vehicles versus ~50-80% for fuel cells) (Whitaker 1994). Besides, the use of hydrogen (H₂) as the fuel in PEM fuel cells are believed to be the most suitable way to meet upcoming future stringent regulations, such as ultra low emissions of NO_x, SO_x, CO, CH₄ and CO₂; e.g. proposal by California government (Creveling 1992). Therefore, H₂ and fuel cells seem to play a significant role as a future potential alternative power generation in reducing the air pollution and increasing efficiency in the energy usage.

A fuel cell is an electrochemical device that directly converts chemical energy into electricity. Since the fuel cells do not have moving parts, such as the blades of turbines, the energy losses due to the friction and other limitations are eliminated, thus resulting in higher thermodynamic efficiency. They produce electrical current for the corresponding voltage across the electrodes as long as there is a supply of a fuel and an oxidant. Therefore, they do not need to be replaced or recharged unlike alkali or rechargeable batteries. A fuel cell basically consists of four parts; gas diffuser/water discharger layer, catalyst coated porous electrodes and an electrolyte.

Hydrogen rich fuel, fed to one side of the fuel cell unit, diffuses through the porous electrode (called anode) to the catalyst (typically platinum) and hydrogen is dissociated on the catalyst to produce hydrogen ions and electrons. While the hydrogen ions diffuse through the electrolyte from the anode to the other electrode (called cathode), electrons flow through an external circuit load (e.g. a lamp) to the cathode electrode. Hydrogen ions and electrons combine with the oxidant (in most cases, air) on the catalyst surface of the cathode porous electrode to form water, which is discharged from the unit with the unreacted oxidant. . Since the voltage of one cell is electrochemically limited to ~1.24 V, the power output can be increased by stacking up the unit cells. The half and the overall cell reactions occurring at the catalyst surfaces of the anode and the cathode are given below;



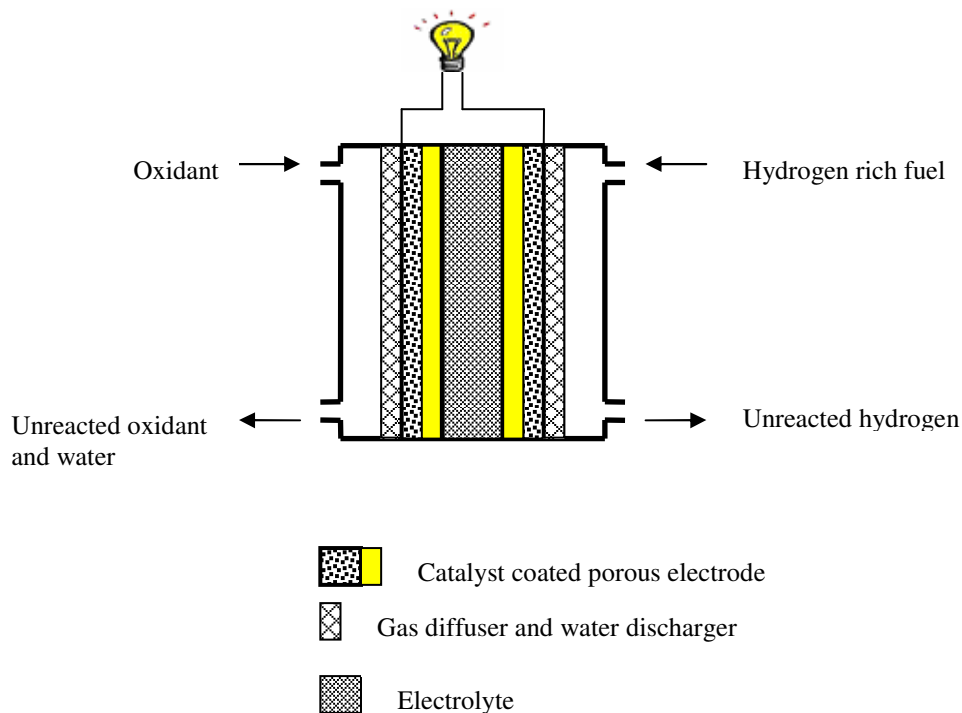


Figure 1.1. The schematic of a fuel cell operating with a hydrogen rich fuel and an oxidant.

There are several types of fuel cells. They are generally named according to their electrolyte used in the cell. Table 1.1 shows their operating temperature range, electrolytes and also their advantages and disadvantages. As seen in Table 1.1, the fuels used for the fuel cells are mostly hydrogen, with the exception of direct methanol fuel cell. Since hydrogen is not freely available in nature, it must be produced using some means.

Electrolysis of water is the best way to produce hydrogen but the overall efficiency is low. Therefore, it is not economical to use water electrolysis at locations where the electricity is not cheap. On the other hand, it is well known that in the petrochemical industry, hydrogen is produced by the gasification and the reformation of fossil fuels (Gary and Handwerk 1994; Simanzhenkoz and Idem 2003). It seems that the use of fossil fuels is economical but it is not environmentally friendly way to produce hydrogen because the by-products could be carbon oxides, nitrogen oxides and sulfur oxides depending on the type of the fuel. To achieve a clean and sustainable production of energy, a new eco-friendly fuel resource is required. In this context, ethanol (a form of biomass resource) satisfies most of these requirements since it is relatively easy to produce from the variety of feed stocks, and also safe to handle, transport and store

(Anthanasio et al. 2004; Cavallaro et al. 2000 and Garcia et al. 2000). The reformation of ethanol to hydrogen unfortunately releases some amount of carbon dioxide as the by-product but the released carbon dioxide could be consumed by the plants, such wheat, as carbon source in their growths hence resulting in a net zero emission of carbon dioxide (Anthanasio 2002). Therefore, ethanol seems to be environmentally sound fuel that can significantly reduce green house gas emissions (Haga et al. 1998). In addition, the use of ethanol does not result in the emission of NO_x, SO_x, particulate matters and other toxic compounds because it is produced using biomass resources.

Table 1.1. Types of fuel cells.

| | Operating temperature (°C) | Electrolyte | Catalyst | Fuel | Fuel cell efficiency (%) | Advantages and disadvantages |
|----------------------------|----------------------------|----------------------------|----------|--|--------------------------|--|
| PEM | 60-100 | Polymer ion exchange film | platinum | Hydrogen (LNG, methanol) | 40-45 | low temp. quick start-up high sensitivity to fuel impurities |
| Phosphoric acid fuel cell | 175-200 | phosphoric acid | platinum | hydrogen (LNG, methanol) | 40-45 | can use impure H ₂ as fuel low current and power large size/weight |
| Molten carbonate fuel cell | 600-1000 | molten carbonate | nickel | hydrogen CO (coal, gas, LNG, methanol) | 45-60 | high efficiency fuel flexibility can use a variety of catalysts high temp. enhances corrosion |
| Solid oxide fuel cell | 600-1000 | yttria-stabilized zirconia | ceramic | hydrogen CO (coal, gas, LNG, methanol) | 50-65 | high efficiency fuel flexibility quick start-up high temp. enhances breakdown of cell components |
| Direct methanol fuel cell | 50-120 | polymer membrane | platinum | methanol | 40 | low operating temp. good for small portable device low performance |

Alternatively, ethanol could be used in combustion related applications, such as internal combustion engines of automobiles, as a fuel additive to supply additional oxygen to achieve complete combustion because it is an oxygenated hydrocarbon. Although little or no carbon monoxide is produced, the combustion related power generation using ethanol is not efficient as mentioned before in this chapter. However, ethanol seems to be a very good energy vector and suitable for fuel cells applications.

H₂ production from ethanol has several advantages when compared with other H₂ production techniques, including the steam reforming of methanol and hydrocarbons. Unlike hydrocarbons, ethanol is easier to reform and is also free of sulfur, which is a catalyst poison in the reforming of hydrocarbons, and also air pollutant (Cavallaro et al. 1996). Unlike methanol, which is highly toxic mainly produced from natural gas, ethanol has low toxicity and could be produced from the variety of biomass resources (Klouz et al. 2002).

Due to the lack of hydrogen fuel infrastructure, recent efforts on developing novel catalysts for the catalytic hydrogen production from hydrocarbons and alcohols have increased significantly and are mainly focused on the reforming of gasoline and methanol in order to utilize the current fuel infrastructure for fuel cell powered vehicles. In contrast, the number of studies on catalytic hydrogen production from ethyl alcohol in literature is less than the publications on methyl alcohol and other hydrocarbons. These studies are basically catalyst screening and have shown that in order for a catalyst to be viable for fuel cell applications, its hydrogen selectivity and the temperature at which it is active are the most important factors to choose the catalyst for fuel cell applications. Hydrogen production from alcohols seems to basically occur through dehydrogenation and decarboxylation reactions. In fact, basic catalysts are known to be very active in the dehydrogenation of alcohols and also the catalysts with moderate oxidation activity could lead to decarboxylation, hence forming hydrogen and carbon oxides (Tanabe K. 1970).

Zinc oxide is known to be mostly basic although there are some weak to moderate acidic sites. Hence, zinc oxide seems to be a good candidate to produce hydrogen from alcohols. However, it is not easy to produce durable zinc oxide catalyst with the surface area which is higher than 100 m²/g. Therefore, an inert oxide could be used to disperse zinc oxide to increase and stabilize its surface area. In addition, basic property of the zinc oxide catalyst could be modified by incorporating copper because copper is moderate oxidizer and also known to be active for water gas shift reaction. In this study silica was chosen as an inert support material to disperse zinc oxide and copper. The objective of this study is to investigate the effects of crystallite size and phases of zinc oxide and copper on the catalytic activity/selectivity in the hydrogen production from ethanol steam reforming. All the catalysts were synthesized using a single step sol-gel and also the precipitation method. The physico-chemical properties

(such as, crystallite size and total surface area) of the catalysts were determined by XRD and N₂ adsorption characterization techniques. The activity tests were performed using a home-made packed bed micro-reactor. Most of the activity tests were conducted at Prof. Erdogan Gulari's laboratory at the University of Michigan, Ann Arbor USA.

This thesis contains five chapters. Following this introduction, a literature survey covering from thermodynamic computational analysis to the experimental studies will be presented in Chapter II. The catalyst preparation procedures, the characterization techniques and also the procedure for the catalytic activity tests will be explained in Chapter III. This will be followed by the presentation and discussion of the results obtained from the catalytic activity/selectivity tests and also the physico-chemical characterization in Chapter IV. Finally, overall conclusions and recommendations will be given in Chapter V.

CHAPTER 2

LITERATURE REVIEW

Thermodynamic analysis on the production of hydrogen from ethanol is necessary to better understand the catalytic performance and the maximum achievable product distribution of a catalyst under a given reaction condition. Therefore, the first part of this chapter will focus on the reaction thermodynamics of ethanol-water systems reported in the literature. This will be followed by summarizing the experimental studies on the catalytic hydrogen production from ethanol and water systems.

2.1 Thermodynamic Analysis Studies

Vasudeva et al. (1996), reported that in all ranges of conditions considered, there was nearly complete conversion of ethanol and only traces of acetaldehyde and ethylene for all ranges of conditions considered in their analysis. For a water- to-ethanol molar ratio in the feed of 20:1, the ratio of moles of hydrogen produced to moles of ethanol consumed was 5.56 compared to the stoichiometric maximum achievable of 6.0. Methane and carbon monoxide also decreased substantially when the water-to-ethanol ratio in the feed was increased from 10 to 20. In addition, for a water-to-ethanol molar ratio of 20:1, increasing in the temperature from 525 to 925°C decreased the equilibrium amounts of methane and carbon dioxide, while increasing the amount of carbon monoxide. The yields of acetaldehyde, ethylene and carbon, which were only in trace quantities, were not affected. For an increase in temperature from 525 to 625 °C the yield of hydrogen initially increased from 5.56 to 5.72 moles per mole of ethanol consumed, and thereafter decreased to 5.17 at 925 °C. Also, they showed that at lower water content (e.g. less than 10 moles of water / mole ethanol) and constant temperature of 725 °C, the yields of methane and carbon monoxide increased with pressure while yield of hydrogen decreased substantially.

Thermodynamic analysis of atmospheric ethanol steam reforming reaction at a temperature range from 600 to 700°C, pressure 1 atm and water to ethanol molar ratio of

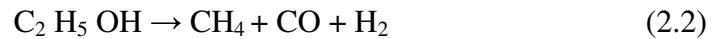
2:1 was investigated by Freni et al. (1996). They observed that thermodynamically favored products were hydrogen, carbon monoxide, methane, acetaldehyde, ethylene and carbon. They also found observed that the amount of hydrogen produced by the ethanol reforming was influenced by the temperature. At 600°C the amount of hydrogen produced was 46.8%, and increased to 58.95% at 700°C. Hydrogen yield was enhanced at low pressures a maximum of 95% of theoretical value was shown to be achievable. Also a high water to ethanol molar ratio in the feed was beneficial to reduce the yield of undesirable products like carbon monoxide, methane and carbon.

Another study is by Garcia and Laborde (1991) and they reported that it was possible to obtain hydrogen by the atmospheric steam reforming of ethanol at temperatures greater than 280°C and methane being an unwanted product. In parallel to previous studies, hydrogen production was found to be favored by high temperature, low pressure and high water-to-ethanol feed ratio. These conditions also reduced the level of by-products significantly. The effects of pressure (1-9atm) on the production of hydrogen and methane were also investigated. The study showed that the hydrogen production increased at all pressures and temperature increased but it increased at a much higher rate at atmospheric pressure and temperature above 327 °C. The study also showed that the concentration of methane in the product stream decreased with the decrease in pressure. For example, at a temperature of 527 °C and a water-to-ethanol feed ratio of 1:1, the methane content at 1 atm was 32% whereas it was 40% for operating pressure at 3 atm. Under a reaction mixture containing a water-to-ethanol molar ratio of 10:1, an operating pressure of 1atm and temperatures, production of hydrogen reached a maximum with minimum CO production above 327 °C while hydrogen to methane ratio increased above 427 °C .

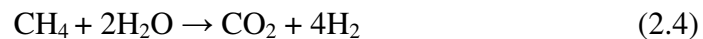
Thoephilus, (2001) studied steam reforming of ethanol in a solid polymer fuel cell at atmospheric condition under a temperature range of 527 to 1027 °C, and water-to-ethanol feed ratios of 3:1 to 6:1. They showed that the ethanol-steam reforming reaction needed to be carried out in two steps: (i) a high-temperature endothermic step (steam reforming), in which ethanol was converted to a gaseous mixtures of H₂, CO, CO₂, CH₄ and unreacted H₂O, (ii) a subsequent, low temperature step (water-gas shift reaction) in which CO is reacted with water to form H₂ and CO₂. Since the shift reaction is equilibrium-limited at high temperatures, CO conversion is not complete and an additional step of CO removal is necessary (e.g. by a preferential CO oxidation

catalyst). It was concluded that hydrogen yield of nearly 100% could be obtained at an optimum condition of water-to-ethanol ratio 5:1 and temperature 727 °C.

Fishtik et al.(2000) used NSTA (nonstoichiometric thermodynamic approach) and acquired a product distribution based on 7 species (ethanol, acetaldehyde, methane, carbon dioxide, hydrogen and water) as a function of temperature at 1 atm for an equimolar ethanol to water feed. Their analysis showed states that the dominant species at low temperatures were methane while at high temperatures, hydrogen was the main product. In addition, STA (stoichiometric thermodynamic approach) was also used in their analysis. They selected a particular limited set of reactions with the most significant contribution to the system's response and predicted the behavior of the system. They pointed out that one important issue with the analysis was that since it was limited to equilibrium conditions the reactions derived could only describes the system's response at equilibrium upon changing the operational parameters. They finally concluded that at low water concentrations, ethanol decomposed according to:



At low temperatures, the reaction 2.1 was favored whereas the reaction 2.2 was faster at high temperatures. They found that at 700-800K, the steam reforming action dominated and with high water:ethanol ratios that promoted water-gas shift reaction and methane steam reforming:



Ioannides et al.(2001) thermodynamically analyzed of hydrogen production from ethanol for SPFC (solid polymer fuel cell) application. The hydrogen generation system consisted of a low-temperature water-gas shift reactor where CO reacts with H₂O producing H₂ and CO₂ following a high-temperature partial oxidation (POX) (and also in some cases; ethanol steam reforming reactor was used instead of POX reactor) and a selective CO oxidation reactor (in order to lower CO below 10 ppm levels). The selective CO oxidation reactor effluent was sent to the solid polymer fuel cell. The SPFC effluent (non-converted hydrogen especially) was recycled back to the reformer

to obtain higher electrical energy conversion efficiencies when a steam reformer was used. So, the system would function under incomplete fuel utilization conditions. Ioannides concluded that because of the recycled hydrogen (to supply the necessary heat to evaporate resulting water required for the reformer, the overall efficiency decreased. Therefore, feeds with water:ethanol ratios greater than 3 had no significant advantage for the steam reforming case. Compared to the maximum of the system with steam reformer, the system with POX reactor gave better maximum hydrogen yield with lower feed ratios. Higher volumetric flow rates were necessary in the systems with POX reactor because due to the low hydrogen concentration (obtained by diluting with nitrogen).

2.2 Catalytic Research

Although there are many studies dealing with methanol steam reforming in the literature; hydrogen production from ethanol ethanol steam reforming and ethanol autothermal reforming has captured the attention of researchers lately.

The ethanol steam reforming reaction over $\text{CuO/ZnO/Al}_2\text{O}_3$ catalyst, and others catalysts, such as NiO/CuO/SiO_2 , $\text{Cu/Zn/Cr/Al}_2\text{O}_3$, $\text{Pt/Al}_2\text{O}_3$, $\text{Pt/La}_2\text{O}_3/\text{Al}_2\text{O}_3$, Pt/TiO_2 , $\text{Pt/MgO/Al}_2\text{O}_3$, Rh/SiO_2 , $\text{Rh/Al}_2\text{O}_3$, and $\text{Rh/MgO/Al}_2\text{O}_3$, was investigated by Cavallaro and Freni (1996). The experiments were carried out in a packed-bed reactor at temperature range of 357 to 477 °C; pressure of 1 atm, water-to-ethanol molar ratio of 6:1 and 10:1. At 377°C, no traces of intermediate products such as acetic acid, acetaldehyde and ethyl acetate were found. However, these compounds were produced at temperatures below 325 °C when the hydrogen and carbon dioxide selectivity was very low. They found that hydrogen, carbon dioxide and carbon monoxide selectivity increased with increase in temperature and also acetic acid selectivity was directly related to the water:ethanol ratio, whereas ethyl acetate selectivity seemed to be related to conversion and temperature. Runs with different space velocities revealed that acetaldehyde was produced in the first step and then was followed by an oxidative step to ester (under slightly excess water) or to acetic acid (under excess water). All catalysts shifted the system towards equilibrium above 360°C. $\text{CuO/ZnO/Al}_2\text{O}_3$ and NiO/CuO/SiO_2 catalysts did not produce coke and/or oxygenated side-products even with water:ethanol ratio lower than 3 although some catalysts required ratios higher

than 4. Noble metal (Pt, Rh) and W-based catalysts showed similar activities as CuO/ZnO/Al₂O₃.

Haga et al. (1998) investigated the effects of crystallite sizes on the activity and selectivity of alumina-supported cobalt catalysts in steam reforming of ethanol under the following reaction conditions: a temperature range of from 223 to 452 °C; the pressure of 1 atm; and water-to-ethanol feed ratio of 4.2:1. They reported that methane, acetaldehyde, ethene, diethyl ether and carbon dioxide were observed as product. The steam reforming of ethanol over cobalt catalysts however proceeded via the formation of acetaldehyde at the temperature below 400 °C. The ethanol conversion reached a maximum value of 100% at 400 °C. Also, the results obtained using different Co initial precursor materials such as cobalt acetate, cobalt carbonyl and cobalt chloride, showed that the activity for ethanol conversion was independent of the starting materials. The production of acetaldehyde steadily increased from lower temperatures and reached a maximum at around 330 °C. Above this temperature, acetaldehyde was converted to carbon dioxide and hydrogen. The carbon monoxide selectivity increased and reached its maximum (53%) at about 380 °C after which it decreased sharply to 23% at 400 °C. Methane selectivity reached a maximum of 20% at 400 °C after which it decreased gradually to 10% at 450 °C.

Marino et al. (1998) studied the activity of γ -alumina supported copper-nickel catalysts for hydrogen production from steam reforming of ethanol at atmospheric pressure and water to ethanol molar ratio of 2.5:1. The effects of the copper loading and calcination temperature on the structure and performance of Cu/Ni/K/ γ -Al₂O₃ catalysts were examined. Copper size increased with the copper loading and also the calcination temperature. The copper loading was varied from 0.00 wt.% to 6.36 wt.%, and the catalysts were calcined at 550 and 800 °C for 5h prior to the activity tests. The reactor effluent gas stream was found to contain H₂, CO, CO₂, CH₄, C₂H₄O, (C₂H₅)₂O, C₂H₅OH and H₂O. The catalysts exhibited acceptable activity, stability and hydrogen selectivity when the reaction was carried out at 300 °C. They concluded that the doping of catalysts with potassium hydroxide neutralized the acidic sites of the support and this way minimized diethyl ether and ethene production. In the catalyst, copper was the active agent; nickel promotes C-C bond rupture and increases hydrogen selectivity and potassium neutralizes the acidic sites of the γ -alumina and improves the general performance of the catalyst. The results of catalyst activity and selectivity measurements together with the findings on the catalyst structure indicated that the

catalyst must have a high dispersion of the active agent in order to maximize ethanol conversion per copper mass unit; the higher copper dispersion was therefore achieved when catalyst was calcined at the lower temperature (550°C).

Ni/La₂O₃ was studied by Fatsikostas et al.(2001) and reported that beyond good long term stability, the catalyst also showed high activity and high hydrogen selectivity. The tests were conducted in a temperature range of 300-800°C by sending a feed of 3:1 water-ethanol ratio at a space time (W/F) range of 0.01 to 0.23 g catalyst.s/cm³. It was also reported that ethanol steam reforming takes place to a significant extent above 400°C due to the test results accomplished at very high space time (0.0375 g catalyst.s/cm³) and only at 700 °C, 100% ethanol conversion was achieved. The dominant reaction at low temperatures was the ethanol dehydrogenation but as acetaldehyde began to reform above 500 °C, its production became less important. No ethylene was produced because La₂O₃ did not have active sites with acidic nature. Carbon monoxide and hydrogen were the only reaction products where carbon dioxide (from water-gas shift reaction) and methane (from methanation reaction) were the by-products at high temperatures. It was also revealed that 100% ethanol conversion and hydrogen selectivity higher than 95% were possible at contact times higher than 0.1 g catalyst.s/cm³. On the other side, time-on-stream data proved the stability of the catalyst only with a little deactivation because of the decrease in ethanol conversion, although there was no significant change in hydrogen selectivity.

Using a feed stream containing stoichiometric amounts of ethanol and water and the following operating conditions: W/F range of 0.018 to 0.105 g catalysts/cm³, and at a temperature range of 600-850 °C, Liguras et al. (2003) reported the effect of types of transition metals, such as Rh, Ru, Pt and Pd and also the metal loading on the activity and selectivity of Al₂O₃, MgO and TiO₂ supported metal catalysts. Complete conversion was obtained at 800° C under severe conditions over 1% Rh/Al₂O₃ catalyst and by-products like acetaldehyde, ethylene (over acidic alumina) and methane from hydrogenation of carbon oxides) were produced with low selectivities. Steam reforming of ethylene caused the selectivity of ethylene decrease to zero (as acetaldehyde) at temperatures ~800°C. Effects of all process parameters are summarized in Table 2.1 for this study. Long term stability test for 5% Ru/Al₂O₃ catalyst revealed that there was no change in hydrogen selectivity (and selectivity to methane, acetaldehyde and ethylene) and decrease in ethanol conversion.

Table 2.1. Effects of process parameters in the study of Liguras et al.

| Parameters | Selectivity / Conversion | Observation |
|--|---|--|
| 1% Me/ γ - Al ₂ O ₃ | X _{C₂H₅OH} | Rh>>Pt>Pd>Ru |
| | S _{H₂} , S _{CO} | Rh>>Pt>Pd=Ru |
| | S _{CO₂} | Especialy Pt,Rh |
| | S _{CH₃CHO} , S _{C₂H₄} | Especialy Rh |
| | S _{CH₄} | Rh, a little |
| 0.5-2 % Rh/ γ - Al ₂ O ₃ 1-5 % Ru/ γ - Al ₂ O ₃ | Increase Rh loading | S _{H₂} , S _{CO₂} ↑ S _{CO} →, S _{byprod} ↓ |
| | Increase Ru loading | S _{H₂} , S _{CO₂} , S _{CO} ↑ S _{byprod} ↓ |
| 5%Ru/ Support | X _{C₂H₅OH} , S _{prod} , S _{byprod} | Al ₂ O ₃ >MgO>TiO ₂ |
| W/F= 0.018-0.105 gcatalyst.s/cm ³ | Increasing W/F | X _{C₂H₅OH} , S _{H₂} , S _{CO} ↑ |

Deluga et al. (2004) have also investigated hydrogen production from autothermal reforming of ethanol using ethanol-water mixtures over ceria supported rhodium catalyst. They have showed that 100% hydrogen selectivity with ethanol conversion greater than 95% could be obtained under space velocities higher than 360000h⁻¹. However, the oxidation reaction was also taking place as the catalyst temperature was reaching about 700°C. Therefore, they reported the runs at 140°C which gave the best activity and selectivity. A simple economic analysis considering an ethanol cycle (starting from photosynthesis and ending in a perfect fuel cell) was also performed. They concluded that for the ideal system the fuel cost (the cost of ethanol to generate electricity) would be about \$0.04 per kWh and suggested that more than 50% of the energy from photosynthesis could be possible to capture as electricity.

The other study related to ethanol steam reforming was investigated by Anthanasio et al. (2002). They used 750°C and water to ethanol molar ratio 3:1 over Ni-based catalyst supported on yittrastabilized- Zirconia (YSZ), La₂O₃, MgO and Al₂O₃. It was reported that Ni/La₂O₃ catalyst exhibited high activity and selectivity towards hydrogen production and also had long term time-on-stream stability of about 100h on stream for the steam reforming of ethanol. The long term stability of Ni/La₂O₃ was attributed to the scavenging of coke deposition on the Ni surface area by lanthanum oxycarbonate species. Results obtained from time-on-stream over Ni/Al₂O₃ catalyst were comparable to those obtained with Ni/ La₂O₃, but the by-product selectivities toward reaction products decreased. In case the of Ni/YSZ catalyst, the selectivity

towards hydrogen was constant; however the selectivity towards CO₂ and CO decreased with time, which became stable only after 20h of time-on stream. Ni/MgO catalyst was very stable under the prevailing conditions, but had poor selective as compared to other catalyst.

Luengo et al. (1992) have studied ethanol steam reforming reaction using Ni, Cu and Cr based catalysts on γ -Al₂O₃ and α -Al₂O₃ supports. The experiments were carried out at a temperature range from 300°C to 550°C; pressure of 1 atm; water-to-ethanol feed ratio of 0.4:1 to 2:1; and ethanol space velocity of 2.5 to 15 h⁻¹. The metallic concentration was chosen to maximize the total conversion but found to increase the selectivity to CO and H₂. γ -Al₂O₃ supported catalysts gave the maximum ethanol conversion of 100% and also the high selectivity to H₂ and CO, unlike γ -Al₂O₃ catalyst in which the ethanol conversion and selectivity to desired product was lower.

In another report by Velu et al. (2002) were studied the steam reforming of ethanol over Cu-Ni-Zn-Al mixed oxide catalyst in the presence or absence of air. The reaction products were H₂, CO, CH₃COOH, CH₃CHO, CH₄ and CO₂. The ethanol conversion increased with increase in O₂/ethanol ratio and reached 100% at the O₂/ethanol ratio of 0.6. Also, the selectivity to CO and CO₂ increased until an O₂/ethanol ratio of 0.4 was reached CO selectivity however dropped at O₂/ethanol ratio of 0.6. Hydrogen yield decreased from 3 mols/mol of ethanol reacted to 2 mols/mole of ethanol reacted in the absence of oxygen. They concluded that the addition of oxygen improved the ethanol conversion and also the oxidation of CH₃CHO to CH₄ and CO₂. It was also reported that Cu-rich catalyst favored the dehydrogenation of ethanol to acetaldehyde, while the addition of nickel to Cu/Al₂O₃ system ruptured the C-C bond, thus enhancing the ethanol gasification and reducing the selectivity to acetaldehyde and acetic acid.

In a recent study, Cavallaro et al. (2003) reported that rhodium impregnated on γ -alumina was highly suitable for the steam-reforming of ethanol. The performance evaluation of Rh/ γ -Al₂O₃ as a reforming catalyst at 650°C showed that the main reaction products were CO₂, CO, CH₄ and CH₃CHO. Also a high conversion of ethanol was obtained at a gas hourly space velocity (GHSV) ranging from 5000 to 80,000h⁻¹, but it decreased as the GHSV was further increased to 300,000h⁻¹. A maximum hydrogen selectivity was obtained at much lower GHSV of 10h⁻¹, which also decreased as the GHSV increased. The catalyst stability was also investigated with and without oxygen. It was observed that catalyst deactivated very fast without oxygen but the

presence of oxygen maintained the catalyst stability and only 10% of activity was lost after 95h of reaction. The addition of oxygen, alternatively, promoted not only metal sintering as a result of hot spot phenomena but also the ethanol conversion through the oxidative dehydrogenation:



Breen et al. (2002) reported the steam reforming of ethanol examined from 400°C to 750 °C over a range of oxide-supported metal catalysts at a water to ethanol molar ratio of 3:1. They concluded that the support played an important role in the steam reforming of ethanol. In fact alumina-supported catalyst were very active at low temperatures for dehydration of ethanol to ethene which at high temperatures (550°C) was converted into H₂, CO and CO₂ as major product and CH₄ as minor product. The activity of the metal was found to be in the order of Rh>Pd>Ni=Pt. Ceria/zirconia supported catalysts were the most active and exhibited 100% conversion of ethanol at a high space velocity and high temperature of 650 °C. The order of activity at higher temperatures was Pt>Rh>Pd. By using combination of a ceria/zirconia-supported metal catalyst with the alumina support, it was observed that the formation of ethene did not inhibit the steam reforming reaction at higher temperatures.

According to Freni et al. (2001), the catalytic activity of alumina (Al₂O₃) was not negligible in the ethanol steam reforming reactions over Rh/Al₂O₃ catalyst when the reaction was carried out at temperature range of 392 to 650°C; pressure of 1.4 atm; and water-to- ethanol feed ratio of 4.2:1 to 8.4:1. They found ethene and water at 347°C and their production increased with temperature and reached equilibrium at 600°C. It was observed that water content did not influence the ethene formation. When 5% Rh was added to alumina, the product analyses below 460°C showed the presence of carbon dioxide, methane and acetaldehyde. The main steam reforming reaction occurred above 460 °C and the products included hydrogen, carbon dioxide, carbon monoxide and methane. The time-on-stream data showed no selectivity changes; however, ethanol conversion decreased with time. This was attributed to the loss of the catalyst dispersion as a result of a size modification of the catalyst particles under the thermal effect of the reaction temperature which caused catalyst grains grow.

Additionally, Freni et al. (2002) examined the steam reforming of ethanol for hydrogen production on Ni/MgO for a molten carbonate fuel cell system. They reported

that the catalyst exhibited very high selectivity to hydrogen and carbon dioxide. The CO methanation and ethanol decomposition were considerably reduced. In addition, coke formation was strongly depressed because of the benefits induced by the use of the basic carrier, which positively modified the electronic properties of Ni.

The study carried out by Galvita et al. (2001) showed that the steam reforming of ethanol for syn-gas production in a two-layer fixed bed catalytic reactor could be viable. The reaction conditions were as follows; a temperature range of from 210°C to 380°C; pressure of 1 atm; and water-to-ethanol feed ratio of 8.1:1 and 1.04:1. In the first bed, the ethanol was converted to a mixture of methane, carbon oxides, and hydrogen over Pd/C catalyst (Pd supported on Sibunit, a special porous carbonaceous material). It was shown that the following two reactions were taking place:



Then this mixture was converted to syn-gas over a Ni-based catalyst for methane steam reforming. It was observed that ethanol conversion increased with increasing temperature, which attained 100% at 330°C and 360°C for water-to-ethanol ratios of 8.1 and 1.04, respectively. They concluded that the use of two-layer fixed-bed reactor prevented the coke formation and provided a yield close to equilibrium.

In a later study of Galvita et al. (2001) characteristics of the Pd catalyst and its catalytic performance in ethanol decomposition in steam were discussed in more detail. TEM micrographs and XP spectra of both fresh and used catalysts showed no difference. In order to identify the intermediate species, the overall reaction mechanism and also the fast and slow steps in the reaction pathway, WHSV was increased from 2200 to 33000 cm³/h-g catalyst. They proposed the following mechanism:



Jordi et al. (2002) examined the hydrogen production process using the steam reforming of ethanol over several cobalt supported catalysts. The reaction temperature was varied from 300°C to 450 °C and water to ethanol molar ratio of 13:1 was used. It

was observed that a negligible steam reforming of ethanol occurred over Co/Al₂O₃ catalyst. The dehydration of ethanol to ethene took place to a large extent. This was attributed to the acidic behavior of Al₂O₃ under similar conditions. Co/MgO catalyst showed low conversion of ethanol of only 30%, and the main reaction was dehydrogenation of ethanol to acetaldehyde. Co/SiO₂ also showed dehydrogenation of ethanol to acetaldehyde as the main reaction. At low temperature, 100% ethanol conversion was obtained on Co/V₂O₅ which ~84% of ethanol converted was through dehydrogenation to acetaldehyde and the rest was the actual ethanol steam reforming. Co/ZnO exhibited the highest catalytic performance among all the catalysts studied. 100% ethanol conversion was achieved and the highest selectivity to hydrogen, and carbon dioxide per mole ethanol reacted were obtained without catalyst deactivation. These experiments revealed that as GHSV increased, the decomposition of ethanol to acetone decreased while the extent of the steam reforming reaction increases. Further increase of GHSV increased the selectivity to acetaldehyde which proved ethanol dehydration to be an intermediate step in ethanol steam reforming.

Aupretre et al. (2002) also studied the effects of types of metals (Rh, Pt, Ni, Cu, Pd, Ru, Zn and Fe) and the role of the supports (γ -Al₂O₃, 12%CeO₂-Al₂O₃, ZrO₂ CeO₂ and Ce_{0.63}Zr_{0.37}O₂) in the steam reforming of ethanol. The experiments were carried at water to ethanol ratio of 3:1 and a constant temperature between 500°C and 800°C and 1 atm pressure. Results of the experiments showed that carbon dioxide was produced in ethanol steam reforming; therefore, metals to be used in active and selective catalysts for ethanol steam reforming should be highly active in steam reforming, and poorly efficient in water-gas shift reaction. To improve the performances of the catalysts in steam reforming, ceria-containing supports were used which enhanced OH surface mobility, and promoted water-gas shift reaction. At 700 °C, γ -Al₂O₃ supported Rh and Ni catalysts appeared to be the most active and selective catalysts in ethanol reforming reaction. Ni/Al₂O₃ gave a higher yield but lower selectivity to CO₂ compared with Rh/Al₂O₃. While concentrating on Rh and Ni catalysts the role of other oxides supports were investigated. Table 2.2 summarizes the results obtained over those catalysts. The results obtained at 600°C showed the catalyst activity in following descending order for Rh; Rh/ Ce_{0.63}Zr_{0.37}O₂>Rh/ CeO₂-Al₂O₃ > Rh/ CeO₂ > Rh/ γ -Al₂O₃. A similar trend was obtained for Ni; Ni/ Ce_{0.63}Zr_{0.37}O₂ > Ni/ CeO₂ > Ni/ CeO₂-Al₂O₃ > Ni/ γ -Al₂O₃. In addition, they reported that Pt, Cu, Zn and Fe catalysts supported on γ -Al₂O₃ was highly active for water-gas shift reaction although they showed moderate activity for steam reforming.

Jose et al. (2003) examined the steam reforming reaction over Ni/Al₂O₃ catalyst. They concluded that temperatures higher than 773 K, high water to ethanol molar ratio (6:1) increased the hydrogen yield (5.2) and selectivity (91%). The excess amount of water in the feed actually enhanced the methane steam reforming while depressing carbon deposition.

Reddy et al. have reported the synthesis of isobutyraldehyde from methanol and ethanol in a single step over CuO/ZnO/Al₂O₃ catalyst where the product distribution of isobutyraldehyde, acetaldehyde, formaldehyde, higher hydrocarbons, acrolein and CO_x was obtained using ethanol and methanol as reactants. In fact, they found that isobutyraldehyde production increased in the following order: Air < air + H₂O < N₂ < N₂ + H₂O. They showed that ZnO promoted CuO/Al₂O₃ was a good ethanol dehydrogenation catalyst and in fact, ethanol was first converted into acetaldehyde which then reacted with methanol to produce isobutyraldehyde.

Table 2.2. Effect of supports on H₂ yield and CO₂ selectivity in the study of Aupretre et al.

| Catalyst | Yield / Selectivity | Catalyst Activity |
|-----------------|----------------------------|---|
| 1% Rh/Support | H ₂ yield | Ce _{0.63} Zr _{0.37} O ₂ >12%CeO ₂ -γ-Al ₂ O ₃ > CeO ₂ >γ-Al ₂ O ₃ |
| | CO ₂ Seletivity | γ-Al ₂ O ₃ >12%CeO ₂ -γ-Al ₂ O ₃ >CeO ₂ > Ce _{0.63} Zr _{0.37} O ₂ |
| 9.7% Ni/Support | H ₂ yield | Ce _{0.63} Zr _{0.37} O ₂ >CeO ₂ > 12%CeO ₂ -γ-Al ₂ O ₃ >γ-Al ₂ O ₃ |
| | CO ₂ Seletivity | γ-Al ₂ O ₃ >12%CeO ₂ -γ-Al ₂ O ₃ >CeO ₂ > Ce _{0.63} Zr _{0.37} O ₂ |

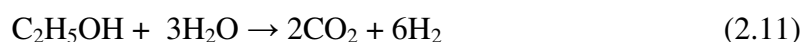
Table 2.3. Mechanisms and Products in the study of Takezawa and Iwasa (1999).

| Feed | Catalyst | Product Distribution |
|---|------------------------------|---|
| CH ₃ CHO / H ₂ O | VIIIB metal/SiO ₂ | CH ₃ OH → CO + H ₂ (main) CH ₃ OH → CO + 2H ₂ → CO ₂ + H ₂ |
| | Cu, Cu/ SiO ₂ | CH ₃ OH →HCHO → HCOOH → CO ₂ + H ₂ |
| C ₂ H ₅ OH / H ₂ O | Cu, Cu/ SiO ₂ | CH ₃ COOH (main), CH ₃ CHO, H ₂ , C ₄ . species |
| C ₂ H ₅ OH | Pd, Pt, Ni | CH ₄ , CO, H ₂ , CH ₃ CHO C ₂ H ₅ OH → CH ₃ CHO + H ₂ CH ₃ CHO → CH ₄ + CO |

Iwasa et al. (1999) reported acetaldehyde production at low conversion levels and at high space velocities over Pd-Zn, Pd-Ga and Pd-In alloys of Pd catalysts as also produced over Cu/ZnO catalyst. Some decrease in acetaldehyde selectivity occurred in the formation of ethyl acetate at higher temperatures and lower space velocities, thus suggesting that ethyl acetate was produced through acetaldehyde despite the decomposition of ethanol to CO and CH₄ Over metallic Pd. Iwasa et al. (1999) have also pointed out the effects of different methods of catalyst preparation on catalytic activities.

In a the comprehensive study carried out by Jordi et al. (2001), various metallic oxides, such as MgO, γ -Al₂O₃, TiO₂, V₂O₅, CeO₂, ZnO, Sm₂O₃, La₂O₃, and SiO₂, were used in the steam reforming of ethanol at temperatures between 300°C and 450°C. The ethanol conversion increased with temperature in all cases. However, significant differences were observed in terms of activity, stability and selectivity of the catalysts. It was observed that γ -Al₂O₃ and V₂O₅ although showed high conversion of ethanol, at lower temperatures (e.g. 350°C), they were not suitable for H₂ production as both were highly selective to ethylene production by the dehydration of ethanol (being acidic in nature). The results also showed that MgO and SiO₂ gave total conversion less than 10% and were also selective for dehydrogenation of ethanol to form acetaldehyde. Similarly, La₂O₃ and CeO₂ gave total conversion of approximately 20%. Other oxides such as TiO₂ and Sm₂O₃ showed high deactivation (conversions dropped from 100% to 3.9% and from 67.2% to 37.2% respectively). After the reaction, these catalysts appeared black. This was attributed to the carbon deposition during the reaction, which could have been responsible for the drop in activity of the catalyst. ZnO reportedly enhanced the steam reforming of ethanol, and showed a high selectivity for to H₂ and CO₂. They concluded that a ethanol is capable of forming wide range of products could be obtained from ethanol reforming. They reported that the product selectivity obtained with different catalysts could be explained with following reactions:

- Ethanol steam reforming:



- Ethanol decomposition to methane:



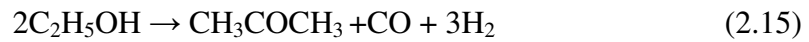
- Ethanol dehydration:



- Ethanol dehydrogenation:



- Ethanol decomposition to acetone:



- Water-gas shift reaction:



Methane, acetaldehyde, acetone, ethene, were all undesirable products because they competed with H₂ for the hydrogen atoms.

Senkan et al. (2005) have investigated the effect of 42 elements from the periodic table supported on γ -Al₂O₃, TiO₂, CeO₂ and Y-ZrO₂ and also the effect of the metal loading (0.5-5 wt%) on the catalytic performance for ethanol steam reforming. They conducted the experiments using a feed stream contained ethanol and water 1:6 mol ratios and at GHSV of 60000 h⁻¹ at 300⁰C, 1 atm. Pt/TiO₂ and Pt/CeO₂ were the most active catalysts (giving the highest ethanol conversions (+90%) and ~30% hydrogen selectivity among all the single component catalytic materials explored). Ethanol conversions also increased with increasing Pt loading.

CHAPTER 3

MATERIALS AND METHODS

In this study, ZnO/SiO₂ catalysts and copper doped ZnO/SiO₂ catalysts were prepared by a single step sol-gel and precipitation techniques and also characterized using Philips X'Pert diffractometer (XRD), and N₂ adsorption surface area measurement method (using Brunauer-Emmett-Teller (BET) approach). All the catalysts were tested in ethanol steam reforming in a home-made packed-bed reactor.

3.1 Materials

The chemicals used to prepare the catalysts and their purities are shown in Table 3.1. All the chemicals were used without further purification.

Table 3.1. Properties of chemicals used in experiments.

| Chemicals | Properties |
|--------------------------------|---|
| Ethanol | Acro Inc.; 200 proof, 99.5% |
| Tetraethyl orthosilicate | Sigma-Aldrich Inc.; 99.99% |
| Zinc nitrate hexahydrate | Sigma-Aldrich Inc.; with 98% |
| Ammonium hydroxide | Sigma-Aldrich Inc.; with 29.3% of NH ₃ |
| Copper (II) nitrate trihydrate | Sigma-Aldrich Inc.; 99.5% |
| Hydrochloric acid | Sigma-Aldrich Inc.; 37% |

3.2 Methods

3.2.1 The Preparation of the Catalysts

3.2.1.1 Oxide Supports

Zinc oxide was chosen to be the main component in all the catalysts and the silica was used to disperse zinc oxide. The precipitation technique was only used to prepare un-doped zinc oxide catalyst whereas the sol-gel method was used to prepare zinc oxide-silica mixed oxides and also un-doped silica.

Sol-gel has been used in the preparation of glasses and ceramics for structural, optical, and electronic applications. It is also a versatile tool for both preparation and understanding of catalytic materials. The method is based on the phase transformation of a sol obtained from metallic alkoxides or organometallic precursors. This sol, which is a solution containing particles in suspension, is polymerized at low temperature to form a wet gel. This one is going to be densified through a thermal annealing to give an inorganic product like a glass, polycrystals or a dry gel. The large variety of available synthetic parameters provides the control of the sol-gel product's structural and chemical properties. This control allows designing for and systematically studying the effects of composition, homogeneity, meta-stable phases, and poring structure on catalytic performance.

The most important advantage of using the sol-gel process is that it offers considerable control over material properties. For single-component oxide, process variables including precursor concentration, pH, and hydrolysis ratio is used to control the important textural and chemical properties of the calcined oxide product ; including surface area, pore size distribution, crystallite size, and surface functionality.

In the preparation of un-doped zinc oxide, zinc nitrate hexahydrate precursor was precipitated using ammonium hydroxide solution at room temperature and the pH of the solution was kept at 10 for one hour. After that, the filtered precipitate was washed twice with de-ionized water at 70°C and then once with room temperature de-ionized water. Finally, the precipitate was vacuum filtered. To obtain un-doped zinc oxide catalyst, the fresh precipitate was dried at 120°C for 24 h and then heated to

500°C at 8°C/min of a heating rate and once 500°C was reached, it was kept at this temperature for 12 h.

The sol-gel procedure given by Wang et al. was modified in this study to prepare the oxide catalysts. The mixed oxide catalysts and their sol-gel preparation parameters are given in Table 3.2. Briefly, tetraethyl orthosilicate was first diluted in some amount of ethanol and then the necessary amount of HCl acid was added. This was followed by adding necessary amount of water and heating the mixture to ~77 °C under total reflux. The mixture was stirred and kept at this temperature for 2 h. At the end of the two hour period, two approaches were followed: In the case of preparing un-doped silica, a necessary amount of ammonia solution was added to the mixture at ~77 °C and the silica gel was obtained in ~10 min whereas in preparing zinc oxide-silica mixed oxides, the required amount of the zinc nitrate precursor was added to the mixture at 77 °C and then 10 min later, the necessary amount of ammonia solution was added. The mixed oxide gel was formed in ~2 h. Finally, all the gels were dried at 120 °C for 24 h and then calcined at 500 °C for 12 h after increasing the temperature of the furnace at 8 °C/min of a heating rate.

Table 3.2. Oxide catalysts and their sol-gel preparation parameters.

| | TEOS | Ethanol | HCl Acid (1 M) | Water | Zn(NO ₃) ₂ .6H ₂ O | Ammonium hydroxide (0.05 M) |
|-------------------------------|----------|-----------|-------------------|----------|---|-----------------------------------|
| Un-doped SiO ₂ | 1.856 mL | 10.798 mL | 6.57 µL | 1.5 mL | 0 g | 0.416 mL |
| 30%ZnO in SiO ₂ | 1.856 mL | 10.798 mL | 6.57 µL | 1.216 mL | 0.7992 g | 0.416 mL |
| 50%ZnO in SiO ₂ | 1.856 mL | 10.798 mL | 6.57 µL | 0.837 mL | 1.8648 g | 0.416 mL |
| | TEOS | Ethanol | HCl Acid (1 M) | Water | Zn(NO ₃) ₂ .0.01H ₂ O | Ammonium hydroxide (0.05 M) |
| 70%ZnO in SiO ₂ | 1.856 mL | 10.798 mL | 6.57 µL | 1.498 mL | 2.7147 g | 0.416 mL |

3.2.1.2 Copper Doped ZnO-SiO₂ Mixed Oxide Catalyst

Copper doped zinc oxide-silica oxide catalysts are designated as Xwt.%Cu-50wt.%ZnO-SiO₂ throughout the text. The amount of ZnO was decided based on the catalytic performance of the ZnO-SiO₂ mixed oxides, as discussed in the results section. Copper loading (i.e. weight % of copper in the catalyst) in the 50 wt%ZnO-SiO₂ catalyst was varied from 5 wt.% to 35 wt.%. The final catalyst formulation for each copper loading (e.g. 5wt.%Cu-(50wt.%ZnO-SiO₂)) was prepared in one pot sol-gel synthesis approach. The same sol-gel method as mentioned in the previous section was used but before adding ammonium hydroxide, the necessary amount of copper (II) nitrate trihydrate was introduced to the mixture. Similarly, the required amounts of tetraethyl orthosilicate, ethanol and HCl acid were mixed at 77°C for 2 h under total reflux and then the necessary amount of the zinc nitrate precursor was added to the mixture at 77°C. The necessary amount of copper nitrate precursor was added to the mixture 10 min later. After 10 min of mixing, the ammonia solution was added at 77°C. The copper doped zinc oxide-silica

Table 3.3. Copper doped zinc oxide silica mixed oxides.

| | TEOS | Ethanol | HCl Acid (1 M) | Water | Zn(NO ₃) ₂ .6H ₂ O | Cu(NO ₃) ₂ .3H ₂ O | Ammonium hydroxide (0.05 M) |
|---------------------------------------|-------------|--------------|----------------------|--------------|--|--|-----------------------------------|
| 5%Cu- 50%ZnO- SiO ₂ | 1.856 mL | 10.798 mL | 6.57 μL | 0.794 mL | 1.8648 g | 0.1911 g | 0.416 mL |
| 15%Cu- 50%ZnO- SiO ₂ | 1.856 mL | 10.798 mL | 6.57 μL | 0.7089 mL | 1.8648 g | 0.5732 g | 0.416 mL |
| 35%Cu- 50%ZnO- SiO ₂ | 1.856 mL | 10.798 mL | 6.57 μL | 0.5388 mL | 1.8648 g | 1.3374 g | 0.416 mL |

mixed oxide gel was formed in ~2 h. The copper doped mixed oxide catalysts and their sol-gel preparation parameters are given in Table 3.3.

3.2.2 Catalyst Characterization

Prepared catalysts were characterized by using two instrumental techniques. The crystalline structures of catalysts, after calcination at 500°C were determined by Philips X'Pert diffractometer (XRD) with CuK α radiation. All the catalysts were scanned from 20° of 2 θ to 90° of 2 θ with a step length of 0.05 of 2 θ .

The surface area and adsorption isotherms of the samples were determined by using the nitrogen adsorption technique over a Micromeritics ASAP 2010 model static volumetric adsorption instrument. Degassing was performed at 400°C for 24 h under 5 μ mHg vacuum.

3.2.3 The Activity Tests of the Catalysts

In this study, a straight Pyrex glass tube (I.D. 4 mm) was used as a micro-reactor. The catalyst inside the tube was supported by a glass wool. The temperature of the catalyst was measured by a K-type thermocouple positioned in such a way that it touched the upper surface of the catalyst bed. In order to eliminate the catalytic effect of the thermocouple, a Pyrex glass tube (with ~0.4 mm of wall thickness) was tightly inserted on the thermocouple. The micro-reactor system was heated by a split high temperature furnace. The temperature of the catalyst was monitored and adjusted automatically by an Omega temperature controller for a given temperature set-point. All the catalysts were ground and sieved to 100-140 mesh size. This particle size range was the minimum attainable for this reactor set-up without causing any excessive pressure drop. The total reactant gas flow rate was adjusted using an argon mass flow controller and the peristaltic pump. Argon gas (99.999% of purity) was used to carry the vaporized ethanol and water mixture that was pumped at a constant flow rate by the peristaltic pump. Ethanol and water mixture was vaporized in a glass bead filled Pyrex evaporator (I.D. 2.54 cm) maintained at 145 °C during the catalytic activity tests. Argon gas and the pump flow rates were adjusted to obtain a reactant feed composition consisted of 1% ethanol and (Water/Ethanol)_{molar}=0 to 15 in the gas phase. Before each run, the peristaltic pump was calibrated using the same ethanol-water mixture while the temperature of the catalyst bed was increased to 500 °C with 50 °C of increment under argon flow. Once 500 °C was reached, peristaltic pump set to a desired flow rate was turned on. All the tests were performed from 500 ° to 300 °C with a 50 °C decrement by

natural cooling of the reactor under the reaction gas mixture. In all the tests, the weight based space velocity was kept at 45,000 mL/h/g (corresponding to $\sim 56,000 \text{ h}^{-1}$ of the gas hourly space velocity). The total gas flow rate and the amount of catalyst was chosen by first checking if there was an external mass transfer limitation in the system. The results on the mass transfer limitation will be given in the results section. The reactor assembly is shown in Figure 3.1.

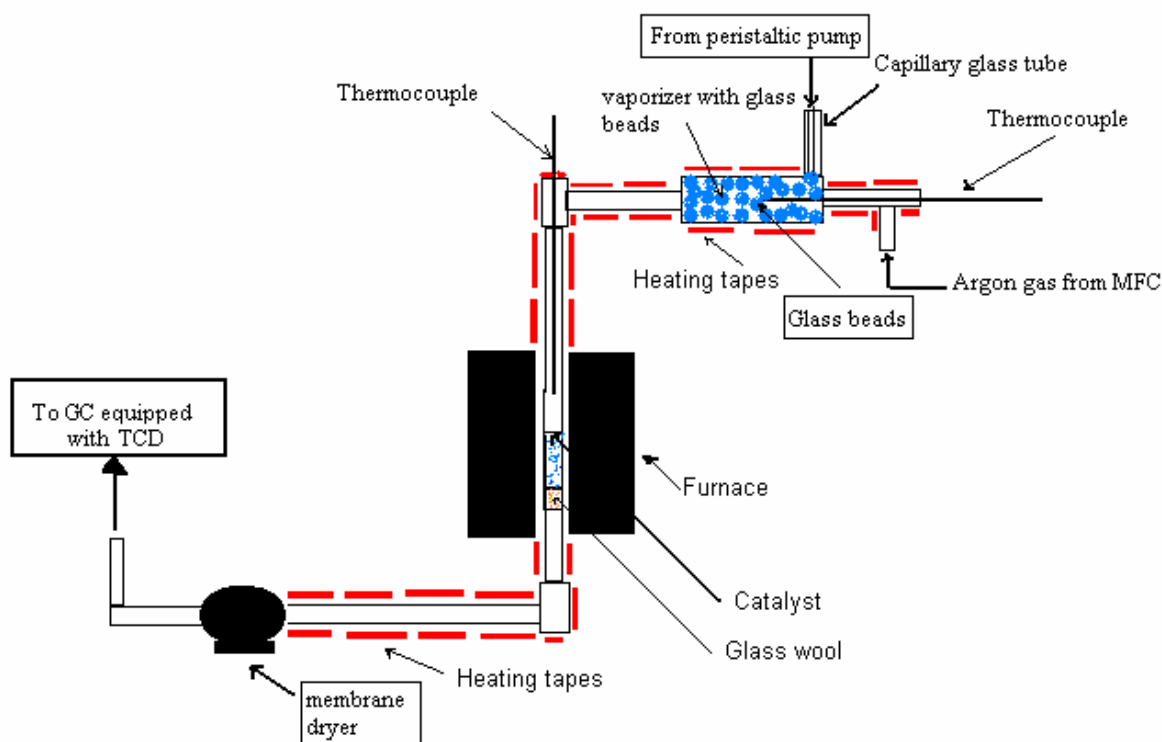


Figure 3.1. Schematic Diagram of the Experimental Setup for the Production of H₂ from Ethanol.

The reactor outlet was analyzed by an online Varian micro-GC CP4900 gas chromatography equipped with two TCD detectors. Varian micro-GC CP4900 gas chromatography had molecular sieve and Porapak Q columns to separate the products for the analysis by the detectors. H₂ concentration was measured using argon as a carrier gas whereas helium was the carrier gas for the other components separated in Porapak Q column. Standard Gas mixtures were used to calibrate the detectors. For each compound, 5-15 data points at each concentration were collected and the average values were used in preparing the calibration curves (the concentration versus the gas

chromatography area). Based on the 95% confidence interval, the error percent in the average area measurement was found to be less than 0.3% for all compounds; for example, the error for a hydrogen concentration measurement was ~0.03% based on 95% confidence interval.

Due to separation difficulties of water and ethanol, the ethanol conversion is calculated using;

$$\text{Ethanol conversion \%} = \frac{\text{total number of moles of carbon in the products}}{\text{total number of carbon in ethanol feed}} \times 100$$

The hydrogen yield and the carbon selectivity reported in this study are defined as;

$$\text{H}_2 \text{ yield} = \frac{\text{number of moles of hydrogen produced}}{\text{number of moles of ethanol converted}}$$

$$\text{Carbon selectivity to the compound, i, (\%)} = \frac{\text{number of moles of carbon in compound, i, produced}}{\text{number of moles of carbon in ethanol converted}} \times 100$$

CHAPTER 4

RESULTS AND DISCUSSIONS

4.1 Characterization Results

BET surface areas of all the catalysts are shown in Table 4.1. For these catalysts, as seen in table, as the amount of ZnO in catalyst increases, BET surface area decreases. Similarly, average pore diameter increases with ZnO loading. Among them, precipitated ZnO shows the lowest total surface area because it is known that ZnO could be easily sintered under the preparation conditions used in this thesis. In fact, these results show that silica stabilizes ZnO in small crystallites when ZnO loading is equal to or lower than 50 wt.%, thus resulting in high BET surface areas.

Table 4.1. BET results.

| Catalyst | BET Surface Area (m ² /g) | BJH Average Pore Diameter (nm) |
|---------------------------|--------------------------------------|--------------------------------|
| SiO ₂ | 887 | 2 |
| 30% ZnO- SiO ₂ | 420 | 2 |
| 50% ZnO- SiO ₂ | 169 | 4 |
| 70% ZnO- SiO ₂ | 112 | 6 |
| Precipitation method | | |
| ZnO | 35 | 2 |

To better understand the effect of ZnO loading, all the catalysts were examined using XRD. The XRD patterns of silica supported ZnO catalysts are shown in Figure 4.1. As seen in Figure 4.1, increasing ZnO loading from 30 to 50 wt% does not reveal XRD peaks corresponding to ZnO crystalline phase although there is a small peak like feature at ~36° of 2θ angle. The small peak like feature is hard to distinguish from silica background contribution. Therefore, it could be safely to assume that ZnO crystallites are less than 5 nm in diameter for 30 and 50 wt% ZnO loadings because XRD analysis is sensitive to crystallite sizes above average 5 nm. However, increasing ZnO loading to 70 wt.% results in XRD pattern corresponding to ZnO crystallite phase. Using Scherrer equation and the reflection at ~36° of 2θ angle, the average ZnO crystallite size was

found to be ~20 nm. In addition, when the XRD spectra of ZnO prepared using the precipitation method is examined, the reflection peaks corresponding to ZnO crystallite phase are seen (it is not shown in Figure 4.1 for simplicity). Similarly, the average ZnO crystallite size was calculated using Scherrer equation and the peak at $\sim 36^\circ$ of 2θ angle. The average crystallite size is ~ 36 nm. In fact, XRD results support BET surface area measurements since the total surface area decreases with increasing crystallite size. Based on the XRD findings, it seems that zinc silicate crystallite phase is not formed under the preparation conditions used in this dissertation. Hence, zinc oxide is mainly dispersed in silica matrix as small crystallites (less than ~ 20 nm) for all zinc oxide loadings.

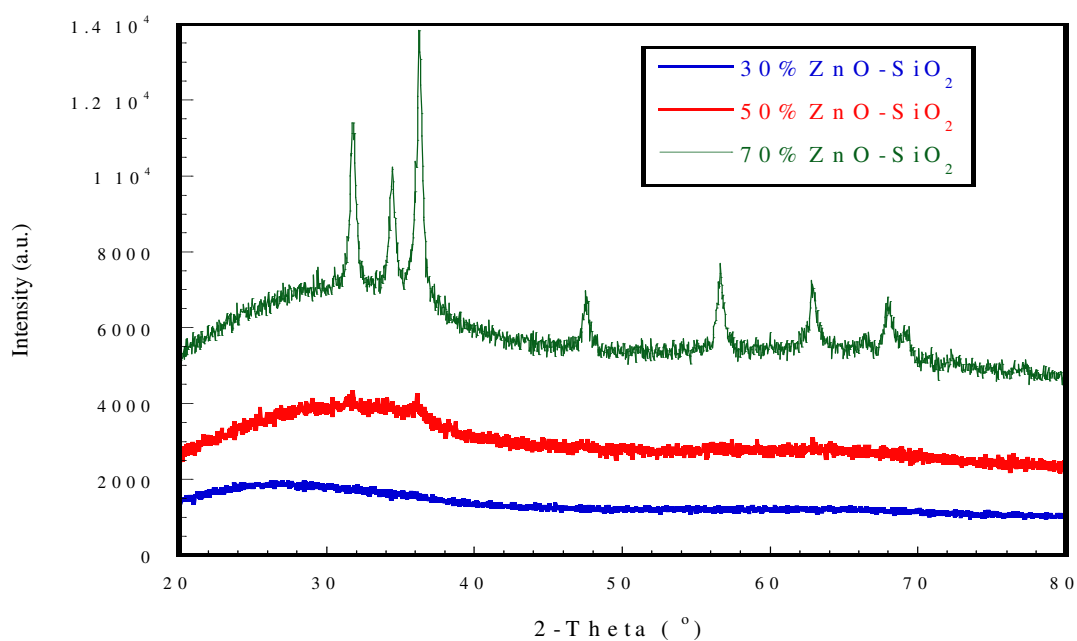


Figure 4.1. XRD spectra of single step sol-gel made catalysts as a function of ZnO loading.

4.2 Catalytic Activity and Selectivity Tests

As explained in Chapter III, all the catalysts were tested in the temperature range of from 300° to 500°C with 50°C increments. In order to be able to have sound comparison of the catalytic activities of all the catalysts, mass transfer limitations were firstly checked. Previous experiences in the catalyst activity tests show that the grain size of the catalyst must be less than $300 \mu\text{m}$ in order to eliminate the internal mass

transfer limitation without causing excessive pressure drop. However, for external mass transfer limitation, the total gas flow rate and the amount of the catalyst must be altered at a maximum temperature in such a way that the space velocity will stay constant for a chosen total gas flow rate and the amount of the catalyst. Therefore, 30%ZnO-SiO₂ catalyst was evaluated for the external mass transfer limitation at 42800 mL/h/g of the space velocity and 500 °C using 1% ethanol, (water/ethanol)_{molar}=12 and argon as balance. These results are shown in Figure 4.2.

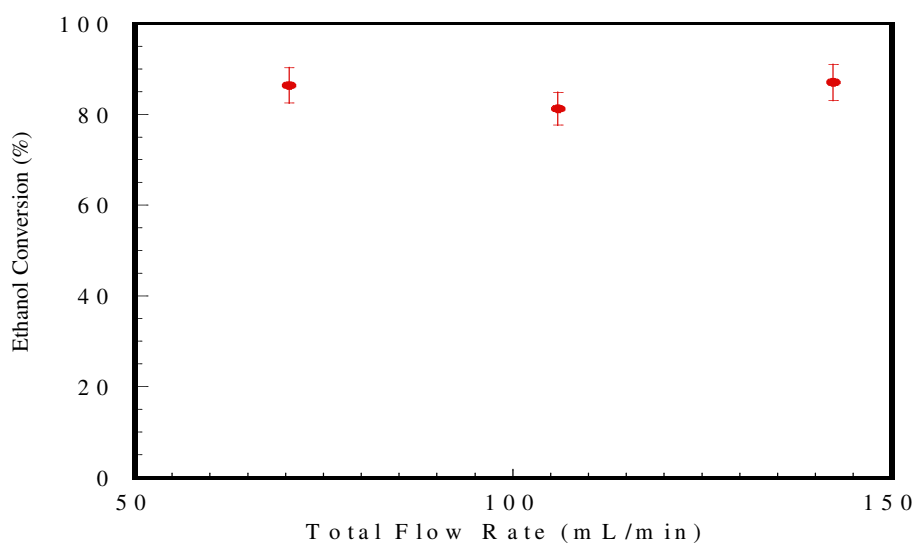


Figure 4.2. Ethanol conversion activity of single step sol-gel made 30%ZnO-SiO₂ catalyst as a function of total flow rate at 42800 mL/h/g of the space velocity and 500°C. Reaction condition: 1% ethanol, (water/ethanol)_{molar}=12, and argon as balance.

Figure 4.2 shows that there was no external mass transfer limitation under the given reaction condition within the experimental error when the total gas flow rate was changed from ~70 mL/min to ~140 mL/min at 42800 mL/h/g of the space velocity.

4.2.1 The Effect of ZnO Loading

It is known that ZnO is very active and selective to hydrogen for the steam reforming of ethanol but it is difficult to obtain a high surface area zinc oxide material

using conventional preparation methods. Indirectly, the surface area of zinc oxide may be increased by dispersing it in an inert support material, such as silica. In fact, this was achieved for all ZnO loadings for ZnO/SiO₂ catalysts. The performances of ZnO/SiO₂ catalysts in ethanol steam reforming reaction were investigated as a function of ZnO loading. Figure 4.3 shows the ethanol conversion as a function of temperature for a set of ZnO loadings.

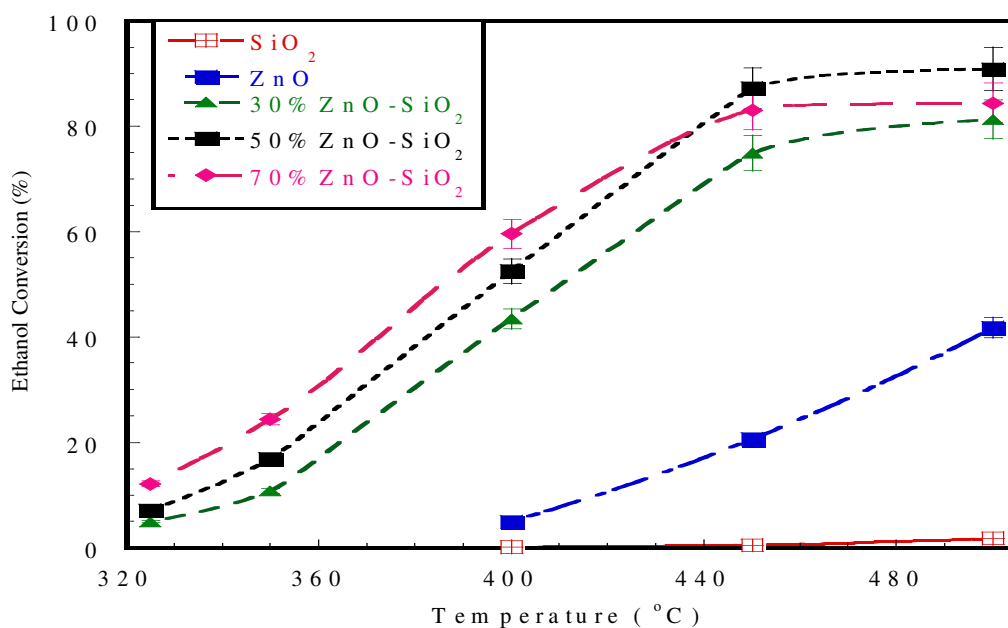
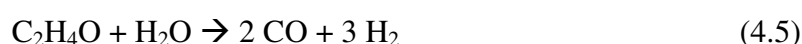
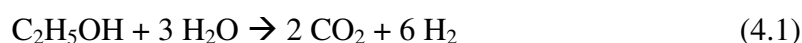


Figure 4.3. Ethanol conversion activities of single step sol-gel made ZnO-SiO₂ catalysts. Reaction conditions: 1% ethanol, (water/ethanol)_{molar}=12, and argon as balance. 0.15 g catalyst and 107 mL/min of total flow rate.

As seen in Figure 4.3, pure silica shows the lowest activity at all temperatures. Similarly, the ethanol conversion over pure zinc oxide catalyst reaches a maximum, ~38%, at 500°C. However, all ZnO/SiO₂ catalysts regardless of zinc oxide loading are more active than pure silica and zinc oxide at all temperatures. For example, at 500°C increasing zinc oxide loading from 30 wt.% to 50 wt.% increases the ethanol conversion from ~80% to ~90% and a further increase of zinc oxide loading to 70 wt.% does not change the ethanol conversion within the experimental error of ~5%. Similar zinc oxide loading effect is also observed at 450°C. However, below 450°C, the activity increases with zinc oxide loadings. Ethanol conversion was the lowest at 320°C and as the temperature was increased, the conversion increased and reached a maximum at 500°C

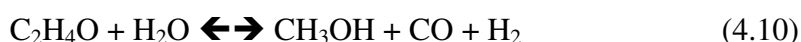
for all zinc oxide loadings. It is known that ZnO is very active and selective to hydrogen for the steam reforming of ethanol but it is difficult to obtain a high surface area zinc oxide material using conventional preparation methods. Indirectly, the surface area of zinc oxide material using can be increased by dispersing in an inert support material. In fact, this was achieved for all ZnO loadings in ZnO/SiO₂ catalysts. Based on the characterization and activity results, it could be speculated that the number of available surface ZnO “*active sites*” increased with increasing ZnO loading from 30 wt% to 50 wt%, hence resulting in high ethanol conversion at all temperatures whereas a further increase of ZnO loading to 70 wt% caused crystallite sintering (as seen in XRD spectra), hence resulting in the decrease of the number of available surface ZnO “*active sites*”. This hypothesis may not seem to work for temperatures between 320°C and 400°C for 50 wt% and 70 wt% ZnO loading as seen in Figure 4.3. This could be due to the possible strong interaction between zinc oxide crystallites and silica matrix, hence affecting the surface properties of zinc oxide crystallites. In order to shed light on the effect of zinc oxide loading, X-Ray Photoelectron Spectroscopy (ESCA) should be used. Unfortunately, ESCA is not available at Izmir Institute of Technology.

From thermodynamically favored ethanol steam reforming reactions are listed below;



As seen in Tables 4.2-4.6, the product distribution analysis shows that the selectivity to ethene decreases as the ZnO loading increases. In other words, the dehydration of ethanol (the reaction 4.2) is favored over silica rich catalysts, such as SiO₂, 30%ZnO-SiO₂ because silica is known to be more acidic than ZnO. For ZnO/SiO₂ catalysts, acetaldehyde is the main product (being higher than 90%) at all temperatures. The major difference between ZnO/SiO₂ catalysts and pure ZnO catalyst is that acetone

is formed over pure ZnO whereas it is not observed over ZnO/SiO₂ catalysts for all ZnO loadings. Acetone over various catalysts was reported to be produced at high temperatures and low space velocities through the aldol condensation reaction in the literature. However, there is no report in the literature if there is a correlation between catalysts' physico-chemical properties and the acetone production selectivity. This study shows that acetone production over ZnO catalysts could be related to the ZnO crystallites and found to increase as ZnO crystallite size and it seems that the average ZnO crystallite must be larger than ~20 nm to produce acetone. In addition, methanol is formed over all the catalysts and the selectivity to methanol is high at low temperatures. Although it is known that ZnO catalyst is active for methanol synthesis from a synthesis gas mixture, methanol may also be formed from acetaldehyde and water through the reaction (4.10) since acetaldehyde is formed at all temperatures and there is water in the feed.



This may explain why hydrogen yield is higher than one at low temperatures for all ZnO loadings because if the dehydrogenation of ethanol is the only reaction occurring at low temperatures, one may expect to get hydrogen yield of one. However, the argument against this explanation is that there is no carbon monoxide observed at low temperatures if the reaction 4.10 is the reaction path to produce methanol. This may be due to low detect ability limit of micro-TCD detectors used to measure CO and also the low amount of methanol produced (30 ppm) (measured with the FID detector) at temperatures less than 350°C.

It is also seen from Tables 4.2-4.6 that CO₂ and CH₄ formations over all ZnO/SiO₂ catalysts increase with temperature. This seems to be due to the water gas shift reaction occurring at high temperatures. In fact, the CH₄ formation over 70%ZnO-SiO₂ catalyst is the highest. CH₄ formation seems to be due to acetaldehyde decomposition (reaction 4.4). In addition, propene is formed over all the catalysts above 400°C. Propene is believed to form through ethene coupling reaction.

Table 4.2. Carbon selectivity to carbon containing products (%) over single step sol-gel made 30%ZnO-SiO₂ catalyst as a function of temperature. Reaction condition: 1% ethanol, (water/ethanol)_{molar}=12, and argon as balance. 0.15 g catalyst and 107 mL/min of total flow rate.

| | CH ₄ | CO | CO ₂ | C ₂ H ₄ | C ₃ H ₆ | C ₂ H ₄ O | Acetone | MeOH |
|-----|-----------------|------|-----------------|-------------------------------|-------------------------------|---------------------------------|---------|------|
| 325 | 0.00 | 0.00 | 0.00 | 2.10 | 0.00 | 96.45 | 0.00 | 1.45 |
| 350 | 0.00 | 0.00 | 0.00 | 2.47 | 0.00 | 95.96 | 0.00 | 1.56 |
| 400 | 0.00 | 0.00 | 0.12 | 3.97 | 0.00 | 95.21 | 0.00 | 0.70 |
| 450 | 0.12 | 0.00 | 0.34 | 3.95 | 0.41 | 94.45 | 0.00 | 0.74 |
| 500 | 1.01 | 0.00 | 1.81 | 3.04 | 1.58 | 92.08 | 0.00 | 0.47 |

Table 4.3. Carbon selectivity to carbon containing products (%) over single step sol-gel made 50%ZnO-SiO₂ catalyst as a function of temperature. Reaction condition: 1% ethanol, (water/ethanol)_{molar}=12, and argon as balance. 0.15 g catalyst and 107 mL/min of total flow rate.

| | CH ₄ | CO | CO ₂ | C ₂ H ₄ | C ₃ H ₆ | C ₂ H ₄ O | Acetone | MeOH |
|-----|-----------------|------|-----------------|-------------------------------|-------------------------------|---------------------------------|---------|------|
| 325 | 0.00 | 0.00 | 0.00 | 1.14 | 0.00 | 97.32 | 0.00 | 1.54 |
| 350 | 0.00 | 0.00 | 0.12 | 1.36 | 0.00 | 97.36 | 0.00 | 1.16 |
| 400 | 0.00 | 0.00 | 0.10 | 2.04 | 0.00 | 97.10 | 0.00 | 0.76 |
| 450 | 0.08 | 0.00 | 0.25 | 2.09 | 0.35 | 96.63 | 0.00 | 0.60 |
| 500 | 0.74 | 0.06 | 1.41 | 2.06 | 1.20 | 94.15 | 0.00 | 0.37 |

Table 4.4. Carbon selectivity to carbon containing products (%) over single step sol-gel made 70%ZnO-SiO₂ catalyst as a function of temperature. Reaction condition: 1% ethanol, (water/ethanol)_{molar}=12, and argon as balance. 0.15 g catalyst and 107 mL/min of total flow rate.

| | CH ₄ | CO | CO ₂ | C ₂ H ₄ | C ₃ H ₆ | C ₂ H ₄ O | Acetone | MeOH |
|-----|-----------------|------|-----------------|-------------------------------|-------------------------------|---------------------------------|---------|------|
| 325 | 0.00 | 0.00 | 0.18 | 0.81 | 0.00 | 97.97 | 0.00 | 1.04 |
| 350 | 0.00 | 0.00 | 0.11 | 1.02 | 0.00 | 97.95 | 0.00 | 0.91 |
| 400 | 0.00 | 0.00 | 0.15 | 1.22 | 0.18 | 97.77 | 0.00 | 0.67 |
| 450 | 0.24 | 0.00 | 0.64 | 1.14 | 0.67 | 96.73 | 0.00 | 0.58 |
| 500 | 2.31 | 0.05 | 3.78 | 1.02 | 1.86 | 90.58 | 0.00 | 0.40 |

Table 4.5. Carbon selectivity to carbon containing products (%) over precipitation made ZnO catalyst as a function of temperature. Reaction condition: 1% ethanol, (water/ethanol)_{molar}=12, and argon as balance. 0.15 g catalyst and 107 mL/min of total flow rate.

| | CH ₄ | CO | CO ₂ | C ₂ H ₄ | C ₃ H ₆ | C ₂ H ₄ O | Acetone | MeOH |
|-----|-----------------|------|-----------------|-------------------------------|-------------------------------|---------------------------------|---------|------|
| 400 | 0.00 | 0.00 | 1.21 | 4.72 | 0.00 | 92.85 | 0.00 | 1.23 |
| 450 | 0.24 | 0.00 | 2.71 | 6.35 | 0.00 | 85.17 | 5.06 | 0.49 |
| 500 | 0.42 | 0.00 | 9.63 | 5.87 | 0.85 | 61.32 | 21.70 | 0.22 |

Table 4.6. Carbon selectivity to carbon containing products (%) and H₂ yield over sol-gel made SiO₂ catalyst at 500 °C. Reaction condition: 1% ethanol, (water/ethanol)_{molar}=12, and argon as balance. 0.15 g catalyst and 107 mL/min of total flow rate.

| | H ₂ Yield | CH ₄ | CO | CO ₂ | C ₂ H ₄ | C ₂ H ₆ | C ₃ H ₆ | C ₂ H ₄ O |
|--------|----------------------|-----------------|------|-----------------|-------------------------------|-------------------------------|-------------------------------|---------------------------------|
| 500 °C | 0.51 | 0.26 | 0.00 | 0.40 | 74.99 | 0.25 | 0.00 | 24.10 |

Table 4.7. H₂ yield over single step sol-gel made 30%ZnO-SiO₂, 50%ZnO-SiO₂, 70%ZnO-SiO₂ and also precipitation ZnO catalysts as a function of temperature. Reaction condition: 1% ethanol, (water/ethanol)_{molar}=12, and argon as balance. 0.15 g catalyst and 107 mL/min of total flow rate.

| | ZnO | 30%ZnO | 50%ZnO | 70%ZnO |
|--------|------|--------|--------|--------|
| 325 °C | | 1.08 | 1.11 | 1.19 |
| 350 °C | | 1.06 | 1.12 | 1.17 |
| 400 °C | 1.23 | 1.17 | 1.16 | 1.23 |
| 450 °C | 1.51 | 1.21 | 1.23 | 1.28 |
| 500 °C | 1.64 | 1.31 | 1.33 | 1.47 |

4.2.2. Water/Ethanol Ratio Effect on the Activity and Selectivity

It was found that 50 wt% ZnO loading among all ZnO loadings seemed to give minimum CH₄ formation and seems to be a good starting candidate in developing a possible ethanol steam reforming catalyst although C₂H₄ formation was high and the water gas shift was low over 50%ZnO catalyst.

The ratio of water to ethanol plays an important role in ethanol steam reforming. The effect of water to ethanol ratio was investigated for the 50%ZnO-SiO₂ catalyst and the results are given in Figure 4.4. It is seen that as the water/ethanol ratio is increased,

the conversion decreases at all the temperatures. In fact, ethanol conversion reaches 95% at H₂O / EtOH ratio of 3 and 6. At the water/ethanol ratio of 12, the ethanol conversion is ~90%. The further increasing the ratio to 15, the ethanol conversion decreases to ~ 84%.

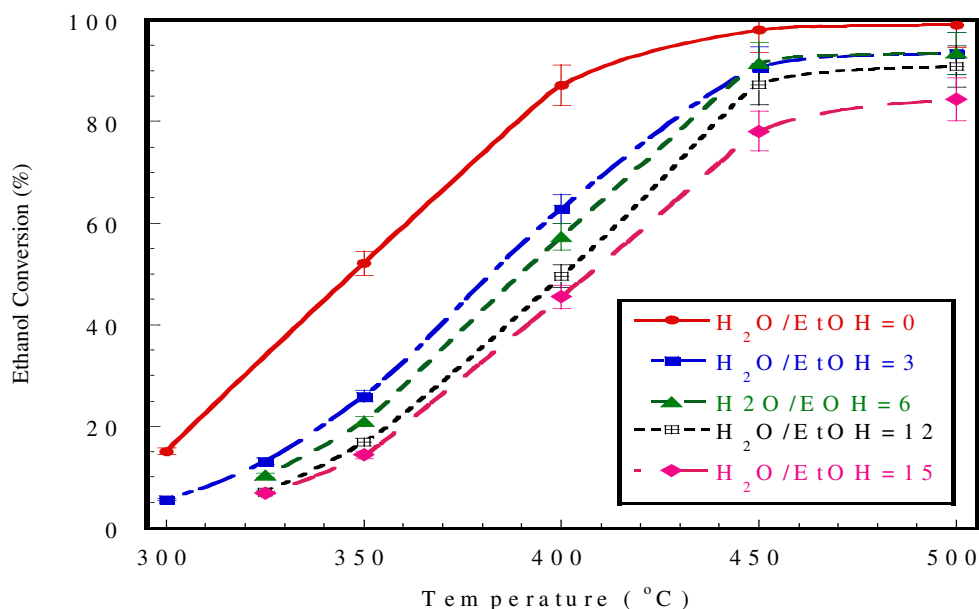


Figure 4.4. Effect of water/ethanol ratio on ethanol conversion activity over single step sol-gel made 50%ZnO-SiO₂ catalyst as a function of temperature. Reaction condition: 1% ethanol, (water/ethanol)_{molar}=0-15, and argon as balance. 0.15 g catalyst and 107 mL/min of total flow rate.

The decrease of ethanol conversion with water/ethanol ratio seems to indicate that water is preferentially adsorbed on the catalyst. In other words, water competes with ethanol for similar “active sites” on the catalyst surface. Since over 50%ZnO catalyst, dehydration and dehydrogenation of ethanol are main reactions, the presence of large amount of water prevents the adsorption of ethanol, hence decreasing the ethanol conversion as water/ethanol ratio increases.

Table 4.8. Carbon selectivity to carbon containing products (%) over single step sol-gel made 50%ZnO-SiO₂ catalyst as a function of water/ethanol ratio and temperature. Reaction condition: 1% ethanol, (water/ethanol)_{molar}=0-15, and argon as balance. 0.15 g catalyst and 107 mL/min of total flow rate.

| (H ₂ O/EtOH) _{molar} | Temp. (°C) | CH ₄ | CO | CO ₂ | C ₂ H ₄ | C ₂ H ₆ | C ₃ H ₆ | C ₂ H ₄ O | CH ₃ OH |
|--|------------|-----------------|------|-----------------|-------------------------------|-------------------------------|-------------------------------|---------------------------------|--------------------|
| 0 | 300 | 0.00 | 0.00 | 0.00 | 1.52 | 0.00 | 0.00 | 98.48 | 0.00 |
| 3 | 325 | 0.00 | 0.00 | 0.16 | 1.43 | 0.00 | 0.00 | 98.28 | 0.13 |
| 6 | 325 | 0.00 | 0.00 | 0.20 | 1.20 | 0.00 | 0.00 | 98.60 | 0.00 |
| 12 | 325 | 0.00 | 0.00 | 0.00 | 1.14 | 0.00 | 0.00 | 97.32 | 1.54 |
| 15 | 325 | 0.00 | 0.00 | 0.00 | 1.03 | 0.00 | 0.00 | 98.36 | 0.61 |
| | | | | | | | | | |
| 0 | 350 | 0.00 | 0.00 | 0.05 | 2.24 | 0.00 | 0.29 | 97.42 | 0.00 |
| 3 | 350 | 0.00 | 0.00 | 0.10 | 1.83 | 0.00 | 0.00 | 97.95 | 0.11 |
| 6 | 350 | 0.00 | 0.00 | 0.13 | 1.62 | 0.00 | 0.00 | 97.97 | 0.27 |
| 12 | 350 | 0.00 | 0.00 | 0.12 | 1.36 | 0.00 | 0.00 | 97.36 | 1.16 |
| 15 | 350 | 0.00 | 0.00 | 0.24 | 1.22 | 0.00 | 0.00 | 98.07 | 0.46 |
| | | | | | | | | | |
| 0 | 400 | 0.05 | 0.00 | 0.08 | 3.70 | 0.05 | 0.49 | 95.62 | 0.00 |
| 3 | 400 | 0.00 | 0.00 | 0.12 | 2.66 | 0.00 | 0.14 | 97.01 | 0.08 |
| 6 | 400 | 0.00 | 0.00 | 0.12 | 2.28 | 0.00 | 0.00 | 97.46 | 0.14 |
| 12 | 400 | 0.00 | 0.00 | 0.10 | 2.04 | 0.00 | 0.00 | 97.10 | 0.76 |
| 15 | 400 | 0.00 | 0.00 | 0.14 | 1.65 | 0.00 | 0.00 | 97.90 | 0.31 |
| | | | | | | | | | |
| 0 | 450 | 0.13 | 0.00 | 0.36 | 5.16 | 0.09 | 1.03 | 93.23 | 0.00 |
| 3 | 450 | 0.15 | 0.00 | 0.42 | 2.81 | 0.00 | 0.51 | 96.08 | 0.04 |
| 6 | 450 | 0.15 | 0.00 | 0.35 | 2.19 | 0.00 | 0.31 | 96.91 | 0.10 |
| 12 | 450 | 0.08 | 0.00 | 0.25 | 2.09 | 0.00 | 0.35 | 96.63 | 0.60 |
| 15 | 450 | 0.15 | 0.00 | 0.39 | 1.80 | 0.00 | 0.15 | 97.27 | 0.25 |
| | | | | | | | | | |
| 0 | 500 | 0.56 | 0.29 | 1.79 | 6.26 | 0.10 | 3.07 | 87.93 | 0.00 |
| 3 | 500 | 0.92 | 0.43 | 1.97 | 2.32 | 0.00 | 1.54 | 92.82 | 0.00 |
| 6 | 500 | 0.80 | 0.44 | 1.54 | 1.87 | 0.00 | 1.05 | 94.20 | 0.11 |
| 12 | 500 | 0.74 | 0.06 | 1.41 | 2.06 | 0.00 | 1.20 | 94.15 | 0.37 |
| 15 | 500 | 1.35 | 0.00 | 2.19 | 1.45 | 0.00 | 0.46 | 94.42 | 0.12 |

Table 4.9. H₂ yield over single step sol-gel made 50%ZnO-SiO₂ catalyst as a function of temperature and water/ethanol ratios. Reaction condition: 1% ethanol, (water/ethanol)_{molar}=0-15, and argon as balance. 0.15 g catalyst and 107 mL/min of total flow rate.

| | (H ₂ O/EtOH) _{molar} =0 | (H ₂ O/EtOH) _{molar} =3 | (H ₂ O/EtOH) _{molar} =6 | (H ₂ O/EtOH) _{molar} =15 |
|-----|---|---|---|--|
| 300 | 1.14 | | | |
| 325 | | 1.12 | 1.10 | 1.15 |
| 350 | 1.20 | 1.14 | 1.14 | 1.19 |
| 400 | 1.21 | 1.16 | 1.17 | 1.14 |
| 450 | 1.24 | 1.19 | 1.20 | 1.24 |
| 500 | 1.32 | 1.30 | 1.29 | 1.33 |

4.2.3. Activity of 50% ZnO-SiO₂ Catalyst as a Function of Cu Loading

ZnO/SiO₂ mixed oxide shows both acidic (Lewis acid) and basic properties. Ethanol dehydrogenation occurs over basic sites of the catalyst which are capable of dissociating H-H and C-H bonds of ethanol. Ethanol dehydration to ethylene, on the other hand, takes place over acidic sites. It has also been shown that over metallic copper, and alumina-, silica- and zinc oxide-supported copper catalysts acetaldehyde and hydrogen can be produced with almost 100% ethanol conversion.

Cu catalysts, especially Cu/ZnO, are known as active catalysts for acetaldehyde hydrogenation. It has also been shown that over metallic copper, and alumina-, silica- and zinc oxide-supported copper catalysts acetaldehyde and hydrogen can be produced with almost 100% ethanol conversion.

Surprisingly, it is found that in all copper loadings, we observe only copper oxide peaks as seen in XRD Figure 4.5. As copper loading is increased, the copper oxide crystallite size shows a dome shaped curve of crystallite thickness (Table 4.10) versus copper loading. At this point, it is not clear if this crystallite thickness behavior is an experimental artifact. Interestingly, XRD spectra show that the presence of copper increases the thickness of ZnO crystallites from <5 nm to above 25 nm for all copper loadings. Small copper oxide crystallite size obtained at 35% copper loading may explain the increase of ethanol conversion observed at high temperatures. The copper oxide crystallite thickness does not have any effect on the carbon selectivity below 450 °C but at 500 °C, the selectivity to CO₂ increases as copper loading is increased to 35%; this may be due to the increased number of sites available at the surface.

Table 4.10. CuO and ZnO crystallite thickness.

| | CuO crystallite thickness | ZnO crystallite thickness |
|-------------------------------|---------------------------|---------------------------|
| 5%Cu-50%ZnO-SiO ₂ | < 5 nm | 26 nm |
| 15%Cu-50%ZnO-SiO ₂ | 22 nm | 43 nm |
| 35%Cu-50%ZnO-SiO ₂ | 9 nm | 25 nm |

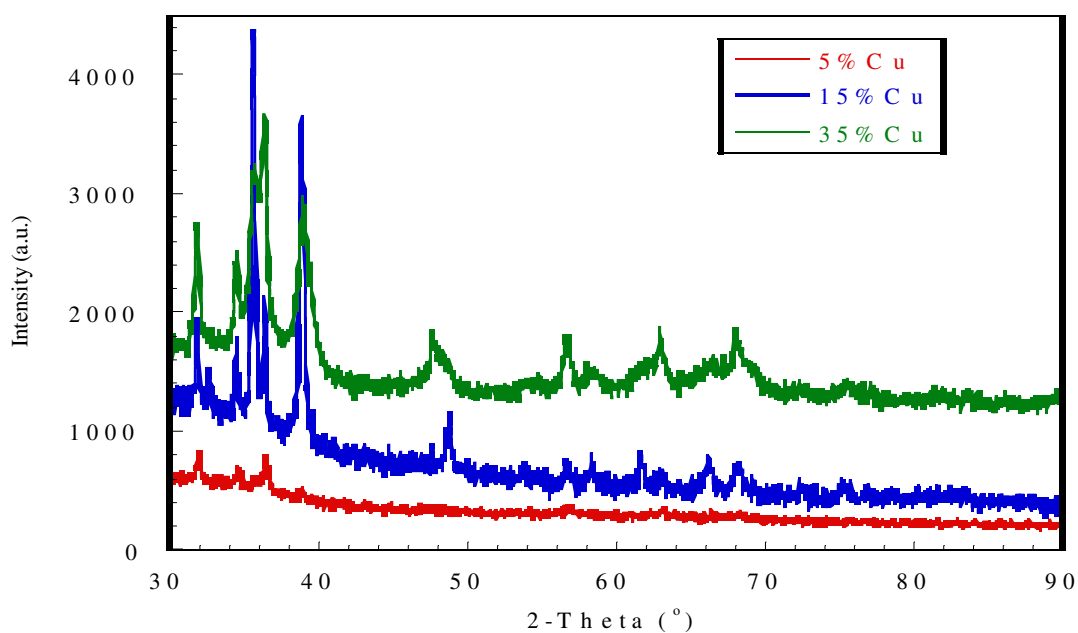


Figure 4.5. XRD spectra of Cu-50%ZnO-SiO₂ catalysts as a function of copper loading.

Figure 4.6 shows the changes in conversion data with respect to temperature over 50%ZnO-SiO₂ catalysts for different loading Cu. The most active catalyst was 35%Cu-50%ZnO-SiO₂ with about 98% conversion of ethanol at the 500°C. At 400°C increasing Cu loading from 5wt% to 35wt% increases the ethanol conversion from ~50% to ~70%. Above 450°C, the activity increases with Cu loading decreases except 35wt% Cu. Ethanol conversion was the lowest at 325°C and as the temperature was increased, the conversion increased and reached a maximum at 500°C for all Cu loadings.

The activities of all catalysts were also evaluated in terms of H₂ yield. In Figure 4.7 effect of copper loading on H₂ yield over Cu-50%ZnO-SiO₂ catalysts as a function of temperature. 5% Cu-50%ZnO-SiO₂ catalyst gave a H₂ yield of 1.28 mol H₂/mol ethanol fed, the yield increased as Cu loading increased and reached maximum of 1.46 mol H₂/mol ethanol fed on 35% Cu-50%ZnO-SiO₂ at 500°C. Since the production of

hydrogen was a major objective in this work, 35% Cu-50%ZnO-SiO₂ catalyst was considered the optimum catalyst. This is because it gave the highest hydrogen yield of 1.46 moles H₂/mol ethanol fed and also had a highest ethanol conversion of 98% at 500°C.

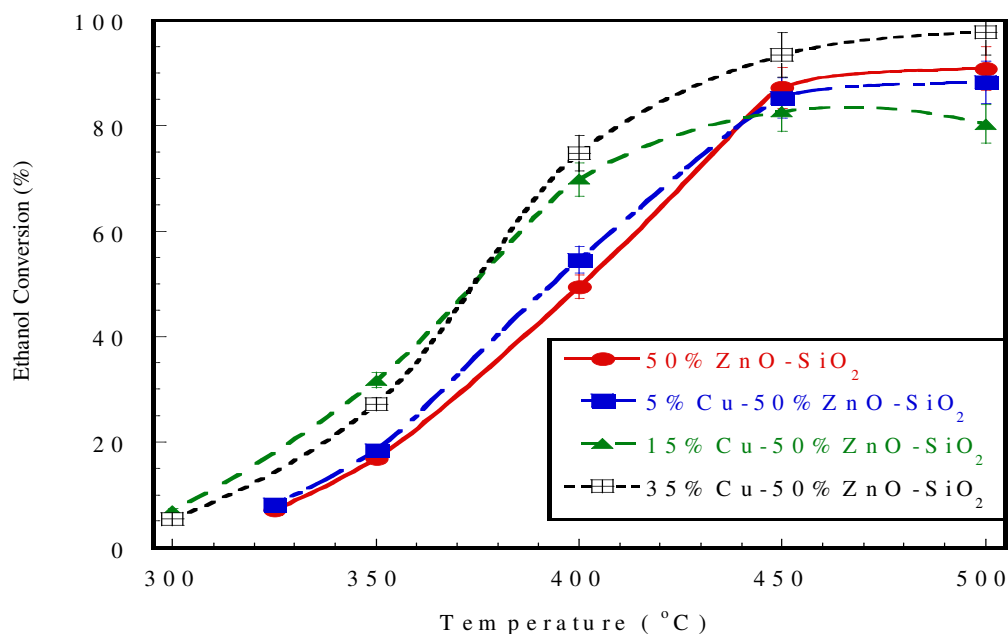


Figure 4.6. Effect of copper loading on ethanol conversion activity over single step sol-gel made Cu-50%ZnO-SiO₂ catalysts as a function of temperature. Reaction condition: 1% ethanol, (water/ethanol)_{molar}=12, and argon as balance. 0.15 g catalyst and 107 mL/min of total flow rate.

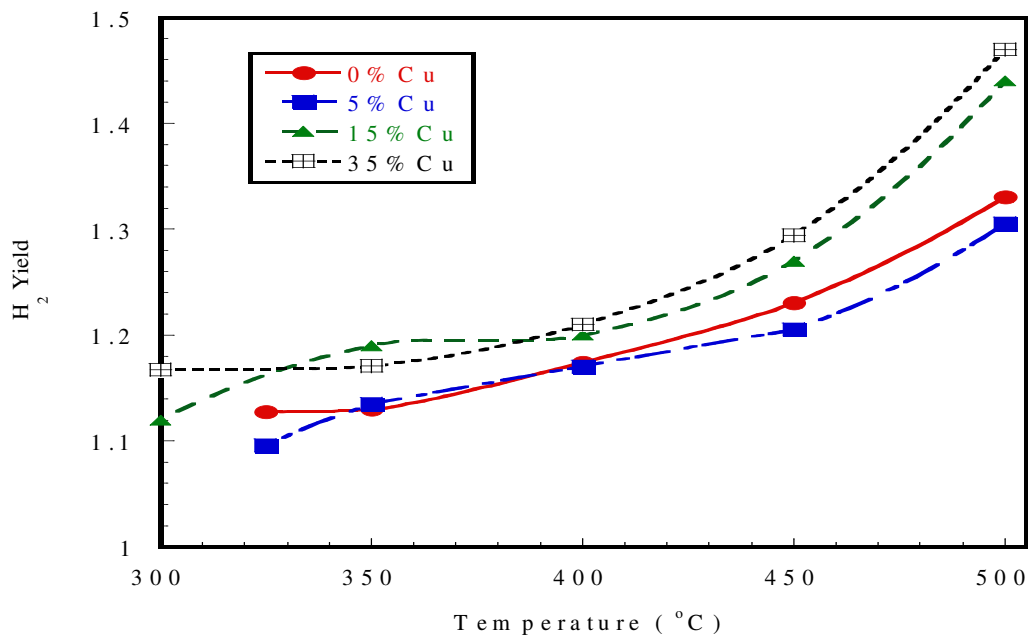


Figure 4.7. Effect of copper loading on H₂ yield over single step sol-gel made Cu-50%ZnO-SiO₂ catalysts as a function of temperature. Reaction condition: 1% ethanol, (water/ethanol)_{molar}=12, and argon as balance. 0.15 g catalyst and 107 mL/min of total flow rate.

The different copper loading 50%ZnO-SiO₂ catalysts are compared in Tables 4.11-4.13 in terms of carbon selectivity to acetaldehyde and temperature. The product distribution analysis shows that the selectivity to ethane increases as the Cu loading increases except 35wt% Cu. For all Cu loadings catalysts, acetaldehyde is the main product at all temperatures. Acetone is formed over all the Cu loading catalysts at 500°C. In addition, methanol is high at low temperatures. Methanol may also be formed from acetaldehyde and water. This may explain why hydrogen yield is higher than one at low temperatures for all Cu loading catalysts because of the dehydrogenation of ethanol is the only reaction occurring at low temperatures, one may expect to get hydrogen yield of one. However, the argument against this explanation is that there is no CO observed below at 500°C. It is also seen from Table 11-13 that CO₂ and CH₄ formations over all Cu loading catalysts. This seems to be due to the water gas shift reaction occurring at all temperature. In fact, the CH₄ formation over 35wt% Cu-ZnO-SiO₂ catalyst is the highest. In addition, propane is formed over all Cu loading catalysts above 400°C.

Table 4.11. Carbon selectivity to carbon containing products (%) over single step sol-gel made 5%Cu-50%ZnO-SiO₂ catalyst as a function of temperature. Reaction condition: 1% ethanol, (water/ethanol)_{molar}=12, and argon as balance. 0.15 g catalyst and 107 mL/min of total flow rate.

| | CH ₄ | CO | CO ₂ | C ₂ H ₄ | C ₃ H ₆ | C ₂ H ₄ O | Acetone | MeOH |
|-----|-----------------|------|-----------------|-------------------------------|-------------------------------|---------------------------------|---------|------|
| 325 | 0.00 | 0.00 | 0.23 | 1.05 | 0.00 | 96.73 | 0.00 | 1.98 |
| 350 | 0.00 | 0.00 | 0.13 | 1.32 | 0.00 | 97.10 | 0.00 | 1.45 |
| 400 | 0.00 | 0.00 | 0.08 | 1.71 | 0.00 | 97.41 | 0.00 | 0.81 |
| 450 | 0.11 | 0.00 | 0.21 | 1.63 | 0.21 | 97.13 | 0.00 | 0.70 |
| 500 | 0.97 | 0.00 | 1.40 | 1.41 | 0.83 | 94.62 | 0.00 | 0.76 |

Table 4.12. Carbon selectivity to carbon containing products (%) over single step sol-gel made 15%Cu-50%ZnO-SiO₂ catalyst as a function of temperature. Reaction condition: 1% ethanol, (water/ethanol)_{molar}=12, and argon as balance. 0.15 g catalyst and 107 mL/min of total flow rate.

| | CH ₄ | CO | CO ₂ | C ₂ H ₄ | C ₃ H ₆ | C ₂ H ₄ O | Acetone | MeOH |
|-----|-----------------|------|-----------------|-------------------------------|-------------------------------|---------------------------------|---------|------|
| 325 | 0.00 | 0.00 | 0.73 | 0.00 | 0.00 | 96.82 | 0.00 | 2.45 |
| 350 | 0.00 | 0.00 | 0.14 | 1.31 | 0.00 | 97.53 | 0.00 | 1.02 |
| 400 | 0.00 | 0.00 | 0.06 | 1.92 | 0.00 | 97.48 | 0.00 | 0.54 |
| 450 | 0.07 | 0.00 | 0.13 | 2.03 | 0.10 | 97.29 | 0.00 | 0.37 |
| 500 | 0.69 | 0.06 | 1.02 | 1.79 | 0.60 | 95.49 | 0.07 | 0.28 |

Table 4.13. Carbon selectivity to carbon containing products (%) over single step sol-gel made 35%Cu-50%ZnO-SiO₂ catalyst as a function of temperature. Reaction condition: 1% ethanol, (water/ethanol)_{molar}=12, and argon as balance. 0.15 g catalyst and 107 mL/min of total flow rate.

| | CH ₄ | CO | CO ₂ | C ₂ H ₄ | C ₃ H ₆ | C ₂ H ₄ O | Acetone | MeOH |
|-----|-----------------|------|-----------------|-------------------------------|-------------------------------|---------------------------------|---------|------|
| 325 | 0.00 | 0.00 | 0.38 | 0.61 | 0.00 | 97.32 | 0.00 | 1.69 |
| 350 | 0.00 | 0.00 | 0.11 | 0.90 | 0.00 | 98.10 | 0.00 | 0.90 |
| 400 | 0.00 | 0.00 | 0.08 | 1.25 | 0.07 | 98.14 | 0.00 | 0.47 |
| 450 | 0.15 | 0.00 | 0.33 | 1.20 | 0.33 | 97.69 | 0.00 | 0.30 |
| 500 | 1.48 | 0.08 | 2.31 | 1.10 | 1.18 | 93.67 | 0.00 | 0.19 |

CHAPTER 5

CONCLUSIONS

Ethanol steam reforming reaction was tested over sol-gel-prepared non-promoted and Cu-promoted zinc oxide catalysts supported on silica in a fixed-bed reactor. Analyses showed similar results with those in the literature. These catalysts acted as ethanol dehydrogenation catalysts in the temperature range of 300-500°C and under other experimental conditions.

In this study firstly, mass transfer limitations were checked before the catalytic activities of all the catalysts were tested. For this reason, both internal and external mass transfer limitations were considered. Previous experiences in the catalyst activity tests show that the grain size of the catalyst must be less than 300 μm in order to eliminate the internal mass transfer limitation without causing excessive pressure drop. It was also found that there were no external mass transfer limitations at total gas flow rates used in this study.

The characterization results obtained by BET and XRD techniques let us assess the following conclusions on the catalysts structure. As the amount of metal used in catalyst increases, BET surface area decreases while average pore diameter also increases. Among synthesized catalysts, precipitated ZnO had the lowest total surface area. XRD analysis of 30% ZnO containing catalyst did not show peaks corresponding to ZnO crystalline phase. Increasing ZnO loading from 30% to 50% did also not reveal peaks of ZnO crystalline phase. However, further increase of ZnO content to 70% showed a XRD pattern corresponding to that of ZnO crystallite phase. Using Scherrer Equation and the peak at $\sim 36^\circ$ of 2θ angle, the average ZnO crystallite size was found to be ~ 20 nm.

In this study, ZnO/SiO₂ catalysts with different ZnO and copper loadings tested for their activity and selectivity in ethanol steam reforming in a packed-bed reactor. According to activity results, pure silica showed the lowest activity at all temperatures. Similarly, the ethanol conversion over pure zinc oxide catalyst reached a maximum, $\sim 38\%$, at 500°C. However, all ZnO/ SiO₂ catalyst regardless of zinc oxide loading were more active than pure silica and zinc oxide at all temperatures. Below 450°C, the activity increased with zinc oxide loadings. Ethanol conversion was the lowest at 320°C

and as the temperature was increased, the conversion increased and reached a maximum at 500°C for all zinc oxide loadings. According to characterization and activity results, it was hypothesized that increase of ZnO loading from 30% to 50% increased the number of available active sites, therefore high ethanol conversion was observed at all temperatures. However, a further increase of ZnO loading to 70% resulted in sintering and the number of available surface ZnO active sites was decreased. In fact, in order to determine the effects of zinc oxide loading more clearly, X-Ray Photoelectron Spectroscopy should be used. Therefore, 50% ZnO/SiO₂ (with ethanol conversion of 90% at 500°C) was found as the most active catalyst among the different ZnO loading.

It was found that the ratio of water to ethanol plays an important role in ethanol steam reforming. The ethanol conversion was 95% at H₂O/EtOH ratio 3 and 6. The reduction of ethanol conversion water/ethanol ratio seems to indicate that there is a preferential adsorption of water on the catalyst. Adsorption of ethanol is prevented because of the presence of large amount of water, therefore ethanol conversion decreases as water/ethanol ratio increases.

Cu catalysts, especially, are known as active catalysts for acetaldehyde hydrogenation. When CuO was used as promoter in 50% ZnO-SiO₂ catalyst, CuO crystallite thickness was found smaller than 5 nm for 5% Cu content. Increase in Cu content from 5 to 15% gave the highest crystalline thickness and it was found as 22 nm. In contrast to this, when Cu content was further increased to 35% crystalline thickness decreased to 9nm. XRD results indicate that for all copper loadings, the thickness of ZnO crystallites is increased from <5 nm to above 25 nm by the presence of the copper. An increase in ethanol conversion at high temperatures may be explained by the small CuO crystallite size obtained at 35% loading. For catalysts with different copper content calcined at the same temperature, ethanol conversion increase as copper loading values increase. Most active catalyst was 35%Cu-50%ZnO- SiO₂ with about 98% conversion of ethanol at the 500°C.

In addition, H₂ yield was used to evaluate activities of all catalysts. The highest H₂ yield (1.46 mol H₂/ mol ethanol at 500°C) was obtained in the case of 35% Cu-50% ZnO-SiO₂ catalyst. Because the main objective of this study was the production of H₂, 35% Cu-50% ZnO-SiO₂ catalyst was found as the optimum catalyst.

We recommend that water gas-shift reaction, acetaldehyde steam reforming and decomposition reactions over 50% ZnO-SiO₂ catalyst should be further studied. With that information of occurring possible reaction of this system can be better explained.

In general, results were obtained in this study similar to with those in the literature reported. Acetone over various catalysts was reported to be produced at high temperatures in the literature. There is no report in the literature about a correlation between catalysts physico-chemical properties and the acetone production. This study shows that acetone production over ZnO catalysts could be related to the ZnO crystallites and found to increase as ZnO crystallite size.

Ethanol is a renewable feedstock. According to studies available in the literature when ethanol is reformed with steam over suitable catalyst, hydrogen can be produced with carbon dioxide; however, no additional carbon dioxide is emitted to the atmosphere, and instead, carbon in ethanol is only recycled in nature to be used again in photosynthesis.

REFERENCES

- Athanasio, N.F. and X.E Verykios, 2004, "Reaction network of steam reforming of ethanol over Ni-based catalysts", *Journal of Catalysis* 225, 439–452.
- Athanasios, N.F. and D.I. Kondarides, 2002, "Production of hydrogen for fuel cells by reformation of biomass-derived ethanol", *Catalysis Today* 75, 145-155.
- Aupretre, F., C. Descorme and D. Duprez, 2002, "Bio-ethanol catalytic steam reforming over supported metal catalyst", *Catalysis Communication* 3, 263-267.
- Breen, J.P., R. Burch and H. M. Coleman, 2002, "Metal-catalyzed steam reforming of ethanol in the production of hydrogen for fuel cell applications", *Applied catalysis B: Environmental* 39, 65-74.
- Cavallaro, S. and S. Freni, 1996, "Ethanol steam reforming in a molten carbonate fuel cell. A preliminary kinetic investigation", *Int. J. Hydrogen Energy* Vol.21, No.6, 465-469.
- Cavallaro, S., V. Chiodo, S. Freni, N. Mondello and F. Frusteri, 2003, "Performance of Rh/Al₂O₃ catalyst in the steam reforming of ethanol: H₂ production for MCFC", *Applied catalysis A: General* 249, 119-128.
- Cheng, W.H., 1995, *Applied Catalysis A: General* 130, 13.
- Choi, Y. and Stenger, H.G., 2002, *Applied Catalysis B: Environmental* 38, 259.
- Cortright, R. D., R. R. Davda and J.A. Dumesic, 2002, "Hydrogen from catalytic reforming of biomass-derived hydrocarbon in liquid water", *Letters to Nature* 418, 964-967.
- Creveling, H. F., , 1992, "Proton Exchange Membrane (PEM) Fuel Cell System R & D for Transportation Applications", *Proc. Annual Automotive Technology Development Contractors' Coordination Meeting, Society of Automotive Engineers*, 485-492.
- Deluga, G.A., Salge, J.R., Schmidt, L.D., Verykios, X.E., 2004, *Science* 303, 993.
- Fatsikostas, A.N., Kondarides, D.I., Verykios, X.E., 2001, *Chemical Communications* 9, 851.
- Fishtik, I., Alexander, A., Datta, R., Geana, D., 2000, *International Journal of Hydrogen Energy* 25, 31.
- Freni, S., 2001, "Rh based catalysts for indirect internal reforming ethanol applications in molten carbonate fuel cells", *Journal of Power Sources* 94, 14-19 .
- Freni, S., G. Maggio, and S.Cavallaro, 1996, "Ethanol steam reforming in a molten carbonate fuel cell: A thermodynamic approach ". *Journal of Power Sources* 62, 67-73.

- Freni, S., S. Cavallaro, N. Mondello and L. Spadaro and F. Frusteri, 2002, "Steam reforming of ethanol on Ni/MgO catalyst: H₂ production for MCFC", *Journal of Power Sources* 108, 53-57.
- Galvita, A.A., G.L. Semin, V.D. Belyaev, V.A. Semikolenov, P.Tsiakaras and V.A. Sobyenin, 2001, "Synthesis gas production by steam reforming of ethanol", *Applied catalysis A: General* 220, 123-127.
- Garcia, E. Y. and M. A. Laborde, 1991, "Hydrogen Production by the Steam Reforming of Ethanol: Thermodynamic Analysis", *Int. J. Hydrogen Energy* Vol.16, No.5, 307-312.
- Garcia, L., R. French, S.Czernik, and E. Chornet, 2000, "Catalytic Steam Reforming of Bio-Oils for the production of Hydrogen: Effects of Catalyst Composition", *Appl. Catal.* 201, 225-239.
- Gary, J.H., G.E. Handwerk, 1994, "Petroleum Refining Technology and Economics", 3rd Edition, (Marcel Dekker, Inc., New York).
- Haga, F., T. Nakajima, K.Yamashita, and S. Mishima, 1997, "Effect of crystallite size on the catalysis of Alumina-supported cobalt catalyst for steam reforming of ethanol", *Reaction Kinetic. Catalysis Letter* Vol.63, No.2, 253-259.
- Ioannides, T., 2001, *Journal of Power Sources* 92, 17.
- Iwasa, N., Yamamoto, O., Tamura, R., Nishikubo, M., Takezawa, N., 1999, *Catalysis Letters* 62, 179.
- Jordi, L. and P. Ramirez, 2001, "Direct production of hydrogen from ethanol aqueous solutions over oxide catalysts", *The royal society of chemistry. Chem. commun.* 641-642.
- Jordi, L., N. Homs, J. Sales and P. Ramirez de la Piscina, 2002, "Efficient Production Of Hydrogen over supported Cobalt Catalysts from Ethanol Reforming" *Journal of Catalysis* 209,306-317.
- Jose, C., F. Marino, M. Laborde and N. Amadeo, 2003, "Bio-ethanol steam reforming on Ni/Al₂O₃ catalyst", *Chemical Engineering Journal*.
- Klouz, V., V.Fierro, P.Denton, H. Katz, J.P. Lisse, S. Bouvot-mauduit and C.Mirodatos, 2002, "Ethanol reforming for hydrogen production in a hybrid electric vehicle: process optimization", *Journal of Power Source* 105, 26-34.
- Liguras, D.K., Kondarides, D.I., Verykios, X.E., 2003, *Applied Catalysis B: Environmental* 43, 345.
- Luengo, C.A., G. Ciampi, M.O. Cencig, C. Steckelberg and M.A Larbode, 1992, "A novel catalyst system for ethanol gasification", *International Journal of Hydrogen Energy* Vol.17, No.9, 667-681.

- Marino, F., E. Cerrella, S. Duhalde, M. Jobbagy and M. Laborde, 1998, "Hydrogen from steam reforming of ethanol. Characterization and performance of copper-nickel supported catalysts", *International Journal of Hydrogen Energy* 23, 1095–1101.
- Reddy, B.M., Reddy, E.P., Manohar, B., 1992, *Journal of the Chemical Society-Chemical Communications* 14.
- Simanzhenkov, V. and R.O. Idem, 2003, "Crude oil chemistry", (Marcel Dekker, New York).
- Takezawa, N. and Iwasa, N., 1997, *Catalysis Today* 36, 45.
- Theophilos, I., 2001, "Thermodynamic analysis of ethanol processors for fuel cell applications", *Journal of Power Sources* 92, 17-25.
- Tsiakaras, P. and Demin, A., 2001, *Journal of Power Sources* 102, 210.
- Vasudeva, K., N. Mitra, P. Umasankar, and S. C. Dhingra, 1996, "Steam Reforming of Ethanol for Hydrogen Production: Thermodynamic Analysis", *International Journal of Hydrogen Energy* Vol.21, No.1, 13-18.
- Velu, S., N. Satoh, and S.C. Gopinath, 2002, "Oxidative reforming of bio-ethanol over CuNiZnAl, mixed oxides catalysts for hydrogen production". *Catalysis Letters* 82, 145-151.
- Whitaker, F. L., 1994, "The Phosphoric Acid PC25™ Fuel Cell Power Plant – and beyond", AIAA 29th Intersoc. Energy Convers. Eng. Conf. (Monterey, CA).